NASA/TP–20210011627

Radio Frequency Plasma Synthesis of Boron Nitride Nanotubes (BNNTs) for Structural Applications: Part III

Stephen J. Hales
Langley Research Center, Hampton, Virginia

Christopher S. Domack
Analytical Mechanics Associates, Inc., Hampton, Virginia

Brian J. Jensen
Langley Research Center, Hampton, Virginia

Peter L. Messick (Retired)
Analytical Mechanics Associates, Inc., Hampton, Virginia

September 2021

NASA STI Program Report Series

Since its founding, NASA has been dedicated to the advancement of aeronautics and space science. The NASA scientific and technical information (STI) program plays a key part in helping NASA maintain this important role.

The NASA STI program operates under the auspices of the Agency Chief Information Officer. It collects, organizes, provides for archiving, and disseminates NASA's STI. The NASA STI program provides access to the NTRS Registered and its public interface, the NASA Technical Reports Server, thus providing one of the largest collections of aeronautical and space science STI in the world. Results are published in both non-NASA channels and by NASA in the NASA STI Report Series, which includes the following report types:

- TECHNICAL PUBLICATION. Reports of completed research or a major significant phase of research that present the results of NASA Programs and include extensive data or theoretical analysis. Includes compilations of significant scientific and technical data and information deemed to be of continuing reference value. NASA counterpart of peer-reviewed formal professional papers but has less stringent limitations on manuscript length and extent of graphic presentations.

- TECHNICAL MEMORANDUM. Scientific and technical findings that are preliminary or of specialized interest, e.g., quick release reports, working papers, and bibliographies that contain minimal annotation. Does not contain extensive analysis.

- CONTRACTOR REPORT. Scientific and technical findings by NASA-sponsored contractors and grantees.

- CONFERENCE PUBLICATION. Collected papers from scientific and technical conferences, symposia, seminars, or other meetings sponsored or co-sponsored by NASA.

- SPECIAL PUBLICATION. Scientific, technical, or historical information from NASA programs, projects, and missions, often concerned with subjects having substantial public interest.

- TECHNICAL TRANSLATION. English-language translations of foreign scientific and technical material pertinent to NASA's mission.

Specialized services also include organizing and publishing research results, distributing specialized research announcements and feeds, providing information desk and personal search support, and enabling data exchange services.

For more information about the NASA STI program, see the following:

- Access the NASA STI program home page at http://www.sti.nasa.gov

- Help desk contact information:

https://www.sti.nasa.gov/sti-contact-form/
and select the "General" help request type.

NASA/TP–20210011627

Radio Frequency Plasma Synthesis of Boron Nitride Nanotubes (BNNTs) for Structural Applications: Part III

Stephen J. Hales
Langley Research Center, Hampton, Virginia

Christopher S. Domack
Analytical Mechanics Associates, Inc., Hampton, Virginia

Brian J. Jensen
Langley Research Center, Hampton, Virginia

Peter L. Messick (Retired)
Analytical Mechanics Associates, Inc., Hampton, Virginia

September 2021

Available from:

NASA STI Program / Mail Stop 148
NASA Langley Research Center
Hampton, VA 23681-2199
Fax: 757-864-6500

Abstract

The emergence of commercial quantities of BNNTs facilitates the exploration of structural material applications. BNNT-reinforced composites must exhibit extraordinary mechanical properties in order to justify the cost premium. Prevailing theory indicates that suitable BNNTs must possess an aspect ratio (AR= *length/diameter*) approaching 10,000 to provide effective discontinuous reinforcement under tensile loading. A survey of commercial products shows that although the quantities are sufficient, lots of uniform morphology are unavailable. Therefore, the opportunity exists to supplement procedures either during synthesis operations or post-synthesis processing in order to deliver homogeneous batches of high AR BNNTs.

An assessment of relevant technologies reveals established methods compatible with sorting of BNNTs by physical dimensions, i.e., size and/or shape. Electrostatic fractionation emerges as the leading candidate, with the potential to isolate high-purity, low-defect, high AR product. The adaptation of existing equipment to the handling of fibrous particulate on the nanoscale will be paramount to success. Although currently focused on BNNTs, the concepts outlined may be applied to nanotubes synthesized from any organic or inorganic compounds. This survey sets the stage for delivering reproducible lots of BNNTs that satisfy the dimensional requirements for use in acreage structural materials.

Table of Contents

Table of Figures

Table of Tables

Symbols and Abbreviations

AC.....alternating current
AR.....aspect ratio
BNNT.....boron nitride nanotube
cm .....centimeters
CNT.....carbon nanotube
CSA.....chlorosulfonic acid
DC.....direct current
d_f .....isolating distance - flakes
d_g.....isolating distance - granules
DMA .....differential mobility analyzer
E.....extraction
f.....flakes
F .....fractionation
g .....granules
H_2O_2 .....hydrogen peroxide
HSPs.....Hansen solubility parameters
kg .....kilograms
kHz.....kilohertz
kV .....kilovolts
LaRC .....Langley Research Center
MMC .....metal matrix composite
$\boldsymbol{M_f}$.....flake mica
µm.....micrometers
nm .....nanometers
P .....purification
PMC .....polymer matrix composite
$\boldsymbol{Q_g}$ .....granular quartz
q_f .....electrostatic net charge - flakes
q_g.....electrostatic net charge - granules
RESAS.....rapid expansion from supercritical to aqueous solutions
RESS .....rapid expansion of supercritical solutions
RFPS.....radio frequency plasma spray
SCF.....supercritical fluid

Introduction

In the mature carbon nanotube (CNT) industry, use in structural applications remains in the incubation phase and the demand for fractionation of product by aspect ratio (AR) has yet to materialize. Therefore, commercial resources have been dedicated to manufacturing efficiency, namely extraction from reactor effluent and removal of by-products. Separation and purification enhancements of in-line processes have deployed cyclonic separators, including electrostatically assisted devices [refs. 1, 2, and 3]. Deploying multiple devices in series, exploratory efforts have also been successful in sorting CNTs by mass or density. Deagglomeration of the resultant entangled masses has been confined to post-synthesis treatments, and the burden has fallen on end users [ref. 4]. Most advances have concentrated on fractionation of CNTs by number of walls or chirality to exploit the superior physical, rather than mechanical, properties [ref. 5].

Historically, research on structural materials has focused on polymer matrix composites (PMCs) discontinuously reinforced with CNTs, and more recently boron nitride nanotubes (BNNTs) [ref. 6]. The allure of BNNTs for reinforcement of metal matrix composites (MMCs) derives from improved compatibility in terms of galvanic corrosion and temperature. As shown in Figure 1, the key attributes are that BNNTs are non-conductive and more thermally stable than CNTs [ref. 7]. The use of BNNT-MMCs as structural materials remains speculative because large batches of uniform, high-AR product are unavailable. Currently, suppliers are not willing to commit resources to more sophisticated fractionation methods until demand for such a product emerges.

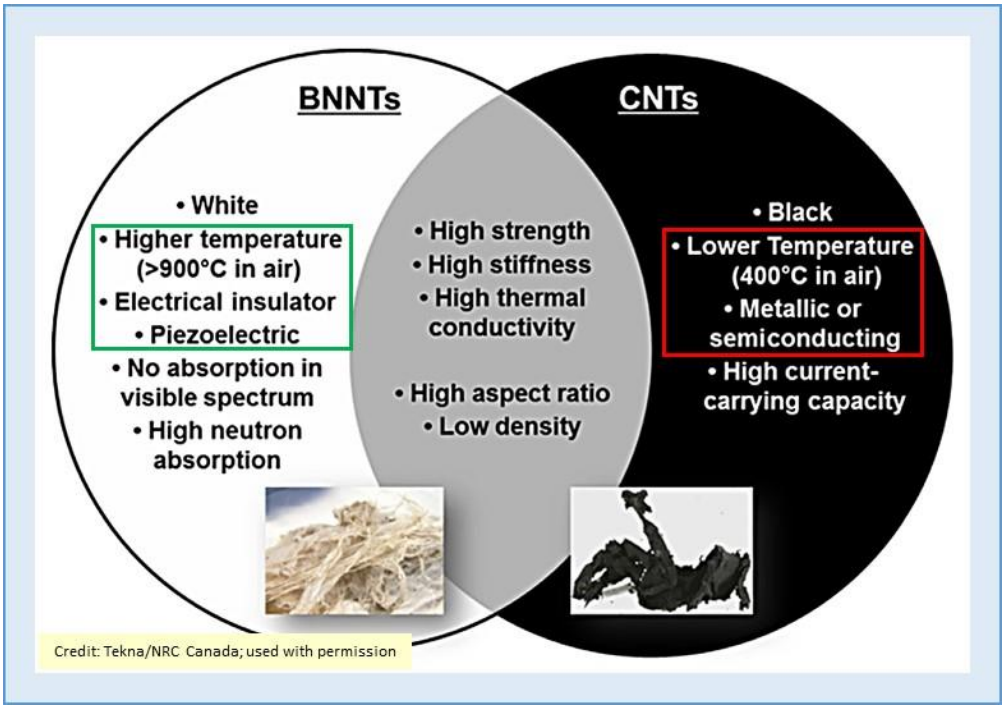

Figure 1. Physical and mechanical properties of BNNTs compared with CNTs [ref. 7]. Note that the high thermal stability and low electrical conductivity enhance the potential for effective reinforcement of MMCs.

The tensile properties of BNNT-MMCs must approach those associated with individual BNNTs to gain traction in aerospace structural applications [ref. 8]. In the case of discontinuously reinforced composites, the established prerequisites for effective matrix reinforcement include

- uniform dispersion
- preferred alignment
- strong interfacial bonding
- high AR

Most of these criteria depend on composite fabrication, but the last criterion is solely dependent on the physical dimensions of the reinforcing agent. Thus, the AR of the constituent BNNTs is projected to play a pivotal role in the mechanical behavior of MMCs, regardless of whether the distribution is aligned or random.

The theoretical relationship between the AR of the reinforcing agent and degree of load transfer to the matrix under tension is illustrated in figure 2 [ref. 9]. Calculations employing the rule of mixtures for modulus or strength enhancement of an aligned, discontinuously reinforced composite reveal that;

- CNTs with any AR contribute to tensile modulus
- only CNTs with an AR ≥ 230 contribute to tensile strength
- an AR $\approx 10{,}000$ is required for a discontinuously reinforced composite to exhibit the tensile properties of its continuously reinforced counterpart

As a consequence, the mean length of masses of ≈ 5 nm-diameter BNNTs destined for structural reinforcement must approach 50 µm to optimize performance.

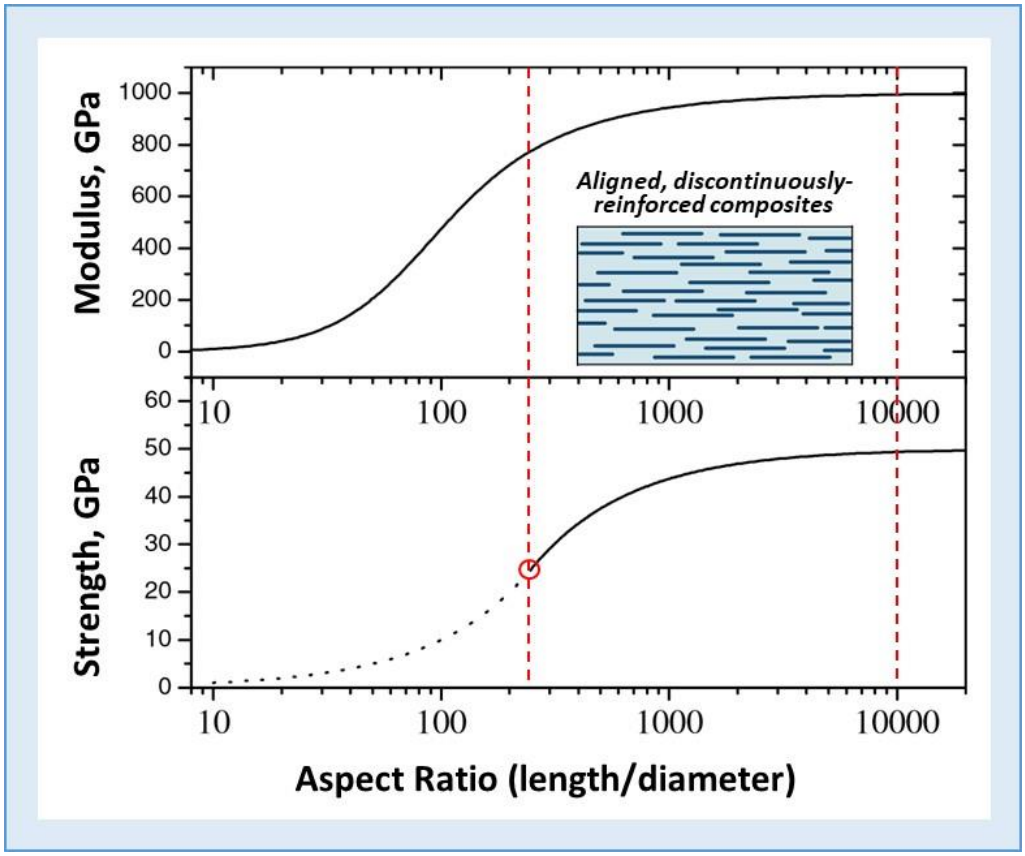

Figure 2. Effect of nanotube morphology on performance of aligned, discontinuously reinforced CNT-PMCs; theoretical increases in tensile modulus and strength of composite with increasing AR of reinforcing agent [ref. 9].

In table 1, the nominal dimensions of high AR BNNTs are compared with the size ranges for common airborne particulate [ref. 10]. The range in diameter is similar to carbon black (10 nm – 0.5 μm), whereas the range in length is similar to "metallurgical dust" (1 nm – 100 μm). Customarily, dust collectors that rely on centrifugal forces are effective for separating particulate in the size range of 0.5 μm to 1 mm, electrostatic in the 1 nm to 50 μm range, and ultrasonic in the 1 nm to 10 μm range. The high AR creates the quandary of whether *diameter* or *length* is the BNNT dimension governing the efficacy of any separation, fractionation, or collection candidate.

Incumbent synthesis techniques tend to yield BNNT product comprising a broad distribution of morphologies and significant impurity content (≥ 10 wt.%) [ref. 11]. Current particle shape fractionation methods tend to be restricted to the isolation of high AR BNNT material in analytical quantities, i.e., micrograms only [ref. 12]. It is evident that shape-based fractionation has yet to be applied to large volumes of nanoparticles, particularly by AR. The incentive for this survey is identification of a processing protocol for collecting high AR, low-defect BNNTs in quantities commensurate with discontinuously reinforced MMCs. The approach adopted builds on proven physical principles conducive to sorting large volumes of non-conductive, non-spherical particles by morphology. The ultimate goal is to rank candidate methods for handling and shape-partitioning of BNNTs produced via induction plasma synthesis.

Table 1. Size ranges of common particles and fibrous particulate compared with established collection methods. Note that high AR nanotubes create a dilemma with regards to the critical dimension that governs separation behavior.

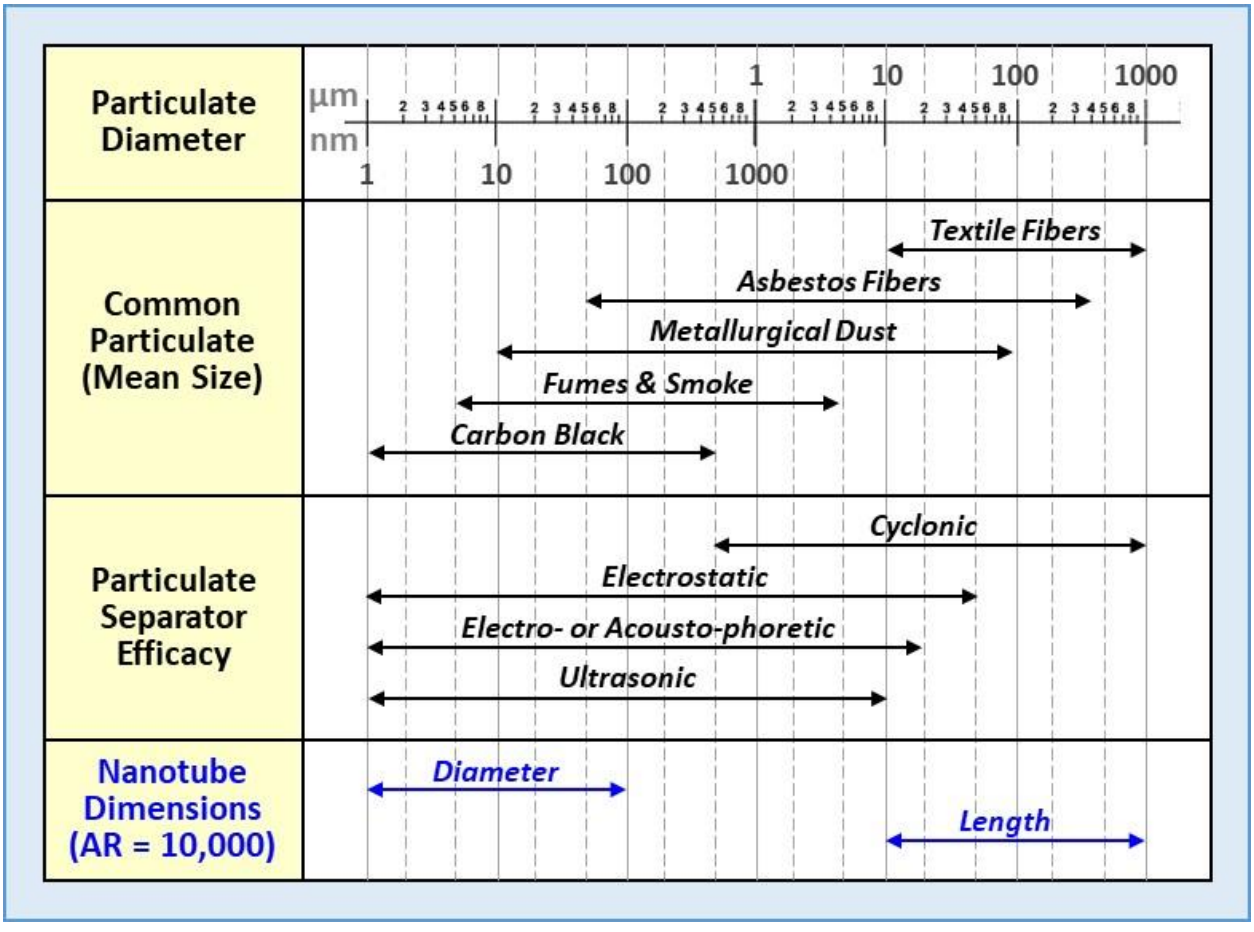

1. Identifying Candidate Methods

The flow chart in figure 3 depicts processing route formulations for sorting of BNNTs manufactured via radio frequency plasma spray (RFPS). BNNTs can be sorted either in-flight upon exiting the reactor, or after being collected as intertwined masses. The elements of the two, fundamentally different routes are dictated by the initial state/condition of the product. During synthesis, the first step is extraction of the BNNT stream from the hot reactor effluent by a continuous, in-line process. Handling involves applying dry methods at elevated temperatures to particulate dispersed in an inert gas. During post-synthesis operations, the first step is deagglomeration of the BNNT bundles by a discontinuous, batch process. Handling involves applying wet methods at ambient temperatures to particulate that has been suspended in a working fluid.

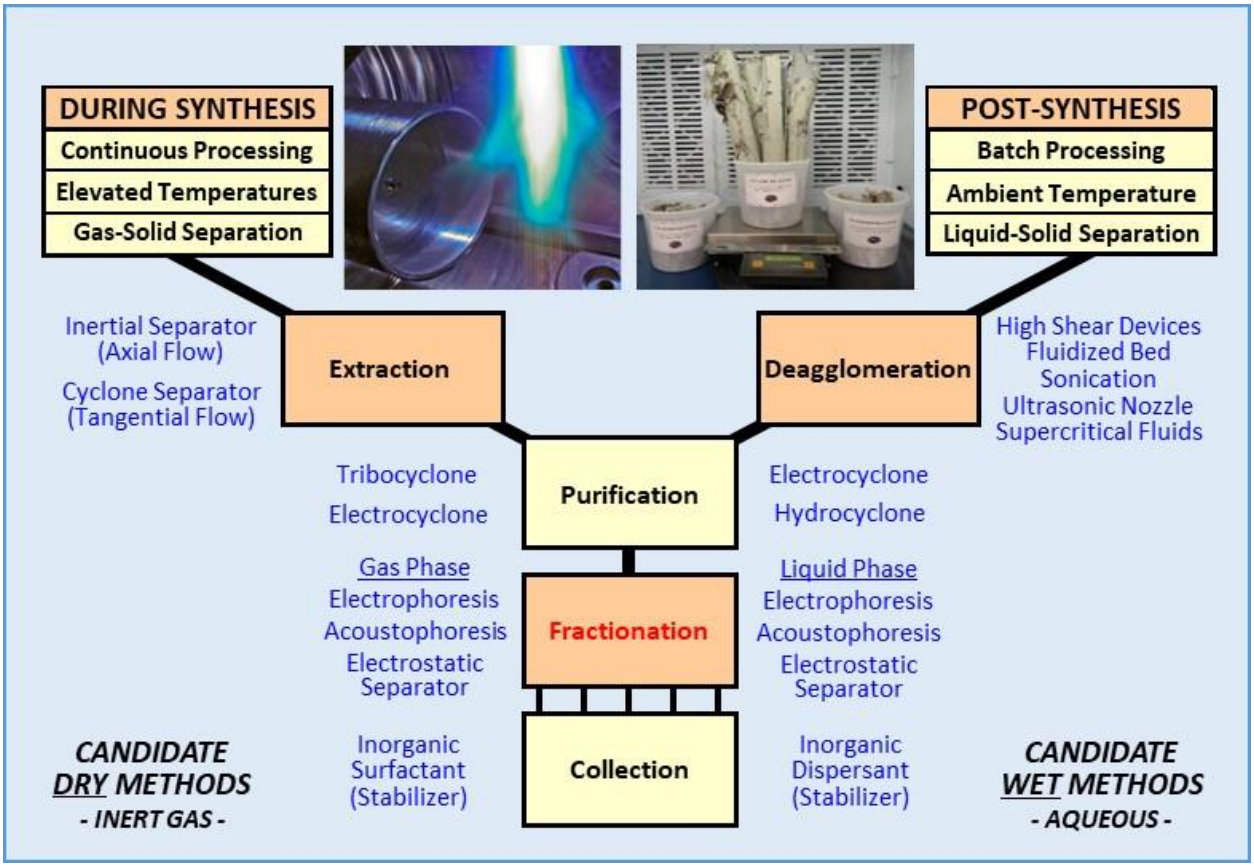

Figure 3. Flow chart outlining potential processing routes for sorting of BNNTs; primarily dry methods during synthesis and wet methods during post-synthesis operations.

Dynamic extraction involves diverting a BNNT-rich stream away from the exhaust gas/by-products and combining with a benign carrier gas. An advantage of this route is that an element of product purification can be introduced early in the proceedings. Static deagglomeration involves untangling BNNTs captured as bulk product and creating a homogeneous suspension in a working fluid. A disadvantage of this route is that achieving a uniform dispersion has proven to be problematic. The subsequent processing steps adhere to a common philosophy, but the operating conditions remain different, i.e., dry vs. wet. Purifying, fractionating, and collecting

the BNNT product requires techniques compatible with gas-solid mixtures via the synthesis route, and vapor-solid or liquid-solid mixtures via the post-synthesis route.

A comparative assessment of technologies identified the candidates that offered the most potential for each stage of the distinctly different routes. The list of dry and wet methods is by no means all-inclusive, but does represent the state of the art. When possible, weight was given to techniques that have proven to minimize damage to CNTs and are amenable to scale-up beyond analytical quantities. In the case of wet methods, priority was also given to techniques capable of operating in an aqueous environment (vapor or liquid) to avoid organic contaminants. The salient features of each of the methods listed are briefly outlined below.

1.1. Extraction Devices

Extraction involves isolating a stream of BNNTs from the reactor effluent during synthesis. The continuous process comprises in-flight separation from hot gases and combination with inert, cold gases for further transport.

1.1.1. Inertial Separator

An example of an inertial separator, also known as a uniflow cyclone, vortex tube, or swirl tube, is shown in figure 4 [ref. 13]. The operating principle is illustrated in figure 4(a) and is similar to cyclonic separators in that particle extraction relies on centrifugal forces. In contrast with most cyclones, devices comprise a tubular geometry with a constant cross-section and the gas/solid mix is introduced axially. A static impeller converts the axial flow of the inlet gas into a vortex flow that creates a particle-rich gas stream adjacent to the outer wall. The gas exiting the tube is split into inner and outer flow paths by concentric outlets.

In such devices, the major central stream is essentially particle-free, and the minor peripheral stream is heavily laden with particles. Inertial separation represents a mature technology for handling fine particulate and is frequently employed for airborne dust removal on jet engine intakes. Process refinements adopted in industrial applications include arrangements of multiple units to increase efficiency and throughput (figure 4(b)) [ref. 13]. The absence of moving parts renders inertial separators particularly compatible with the high temperatures and corrosive environments typical of nanotube synthesis.

1.1.2. Cyclone Separator

Cyclonic separation is a mature technology that has been utilized for capturing fine particulate for decades [ref. 14]. Gas cyclones assume many guises, but all adhere to the same operating principle. The most common devices are of the dry, reverse flow-type depicted in figure 5(a). Cyclone separators have a conical geometry and the gas/solid mix is introduced tangentially [ref. 15]. Inlet gas enters sideways near the top, flows downwards in a helical trajectory, and flows back upwards in the center to be discharged axially or tangentially at the top. Centrifugal forces cause particle impingement on the outer wall and gravity forces the particles to the base of the unit for extraction. As the rotating flow moves towards the narrow end of the cyclone, the rotational radius of the stream decreases, thus separating progressively smaller or lighter particles [ref. 14].

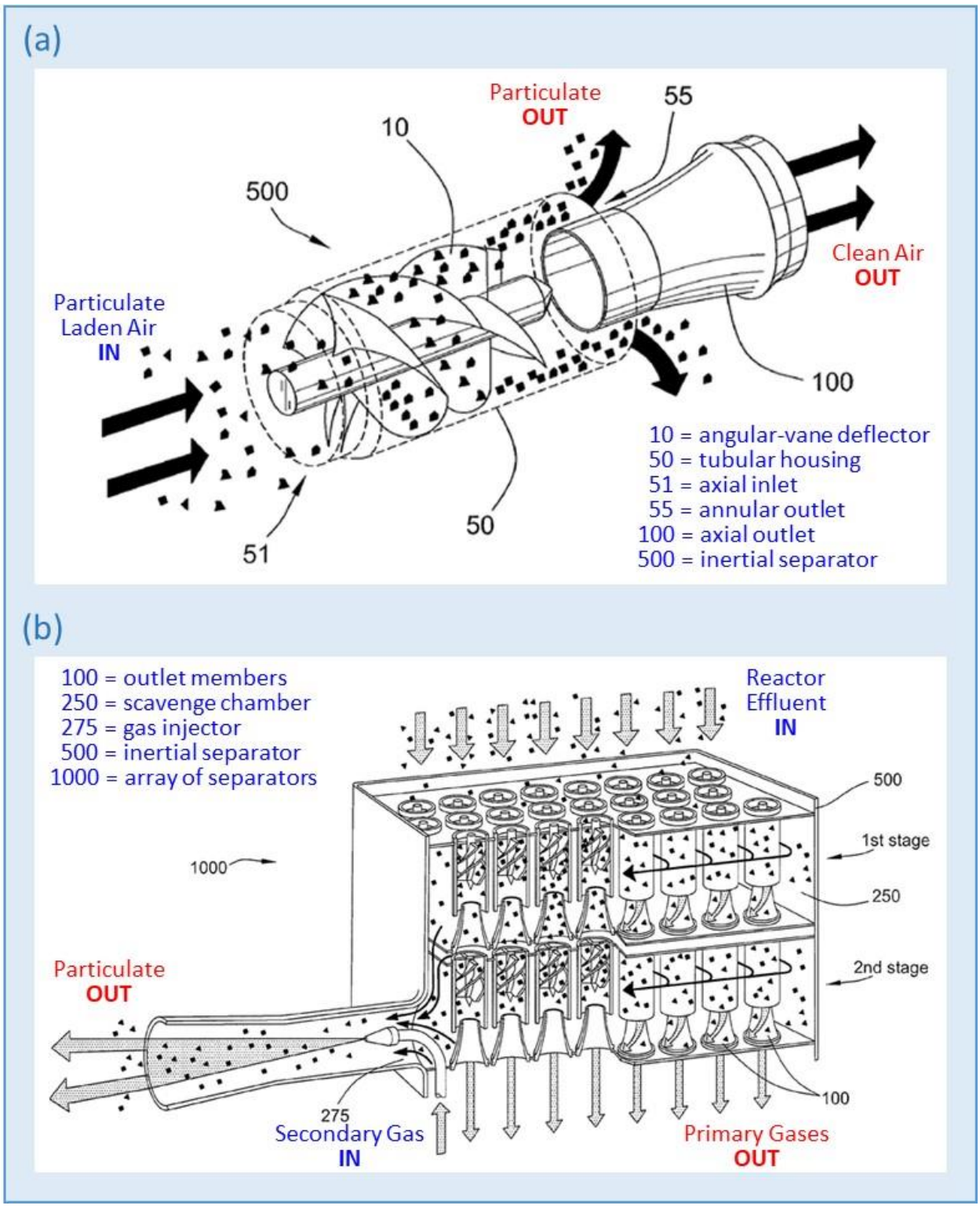

Figure 4. Axial flow, inertial separators [ref. 13]; (a) configuration of single unit; (b) array of multiple units. Note that particulate is scavenged from the effluent stream (primary) and combined with an injected gas flow (secondary).

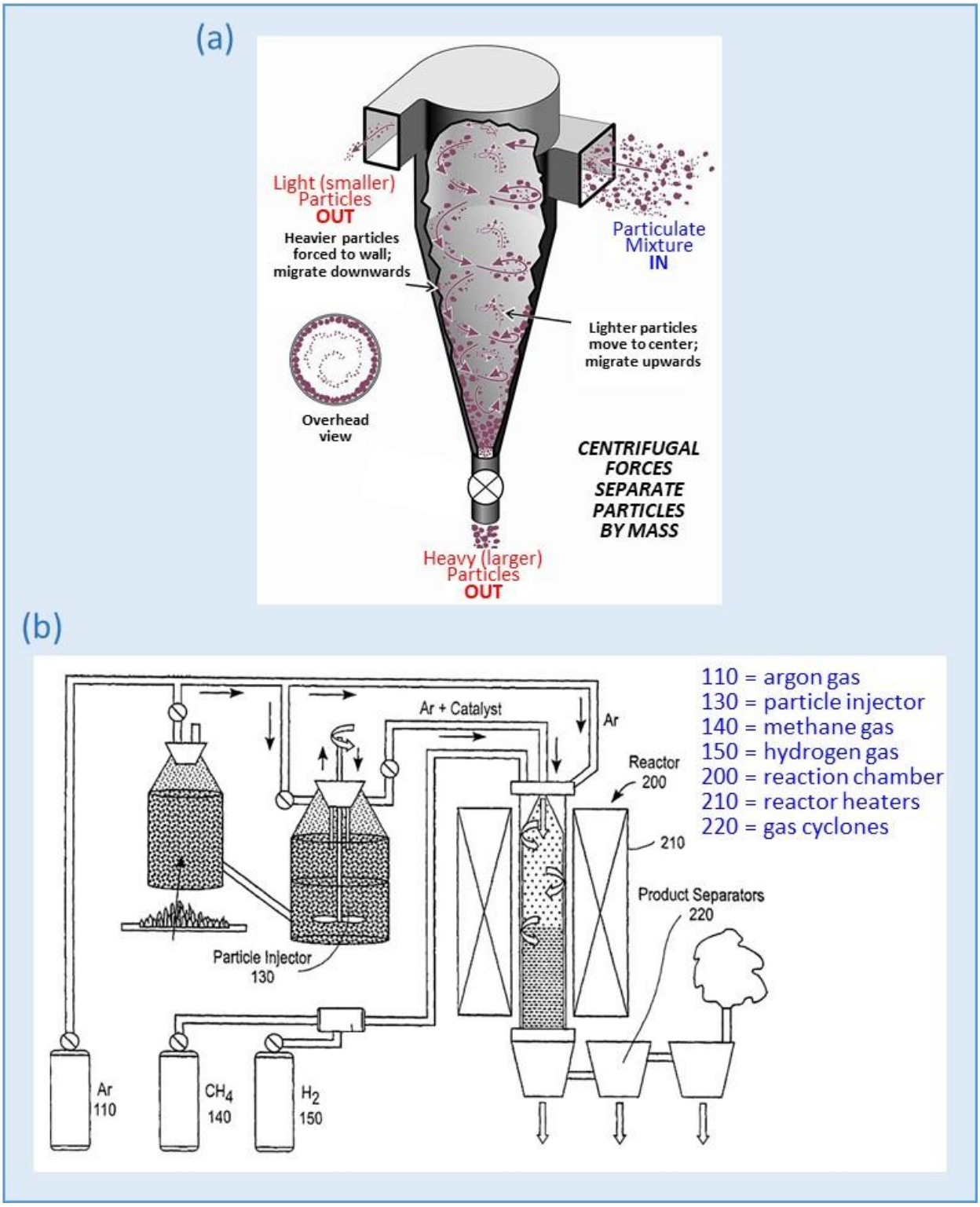

Figure 5. Tangential flow, gas cyclones; (a) typical geometry of individual unit for separating particulate by mass [ref. 15]; (b) multiple units arranged in series (product separators 220) during CNT production [ref. 1].

Cyclone separators are very effective for fibrous particulate and are employed in many industrial environments for dust abatement. Again, the absence of moving parts allows operation in harsh conditions, including elevated temperatures. Collection efficiency can be tailored by adjusting the shape of the separator body with respect to the inlet and outlet dimensions. In combination with volumetric flow rate, the geometry defines the lower limit of the particle size or mass that can be removed [ref. 16]. This feature permits coarse fractionation of particulate when multiple devices are deployed either in series or in parallel. A number of recent patents related to commercial production of CNTs teach in-line separation from reactor effluent using various types of cyclonic devices [refs. 2 and 3] The example shown in figure 5(b) depicts cyclone separators arranged is series for product extraction during synthesis operations [ref. 1].

1.2. Deagglomeration Devices

Deagglomeration involves combining BNNTs with a working fluid in order to achieve homogeneous mixtures on a sub-micron scale. Customarily a batch process, suspension includes mechanical or acoustic agitation to effect fragmentation of aggregates, bundles, or clusters without damaging individual BNNTs.

1.2.1. High Shear Device

The rotor-stator configuration illustrated in figure 6(a) is the most practical among high-shear devices used for mechanical disintegration, mixing, and propulsion of fluid-aggregate mixtures [ref. 17]. A series of rotating blades interacting with fixed heads/screens generate intense hydrodynamic stresses and cavitation that result in deagglomeration [ref. 18]. Large volume mixers can be deployed in either single pass mode for continuous processing, or multi-pass mode for recirculating systems (batch processing) [ref. 19]. Common application includes a multitude of industries where the final product assumes the form of suspensions, slurries, or emulsions [ref. 20]. Examples of commercial devices are shown in figure 6(b), specifically designed for ultra-high-shear processing of nanoparticle suspensions [refs. 21 and 22]. Significantly, uniform dispersions of long CNTs in liquid polymers have been achieved using such high-speed, shear-force mixing devices [ref. 23].

1.2.2. Fluidized Bed

Fluidized beds comprise a mechanical mixture of fluid and solid particles that can be in a broad range of shapes and sizes. Traditionally, the working fluid contains a suspension of fine particles that is continuously agitated and homogeneously expanded by aeration (figure 7(a)) [ref. 24]. The velocity of the upward flow of gas, liquid, or a combination controls the mean size of the particles or agglomerates exiting the reactor (figure 7(b)) [ref. 25]. Such fluidization is used extensively in the pharmaceuticals industry to break-up agglomerates and improve compound homogeneity. The technology has already been applied in-line to control the size of CNT agglomerates produced during synthesis operations [ref. 26].

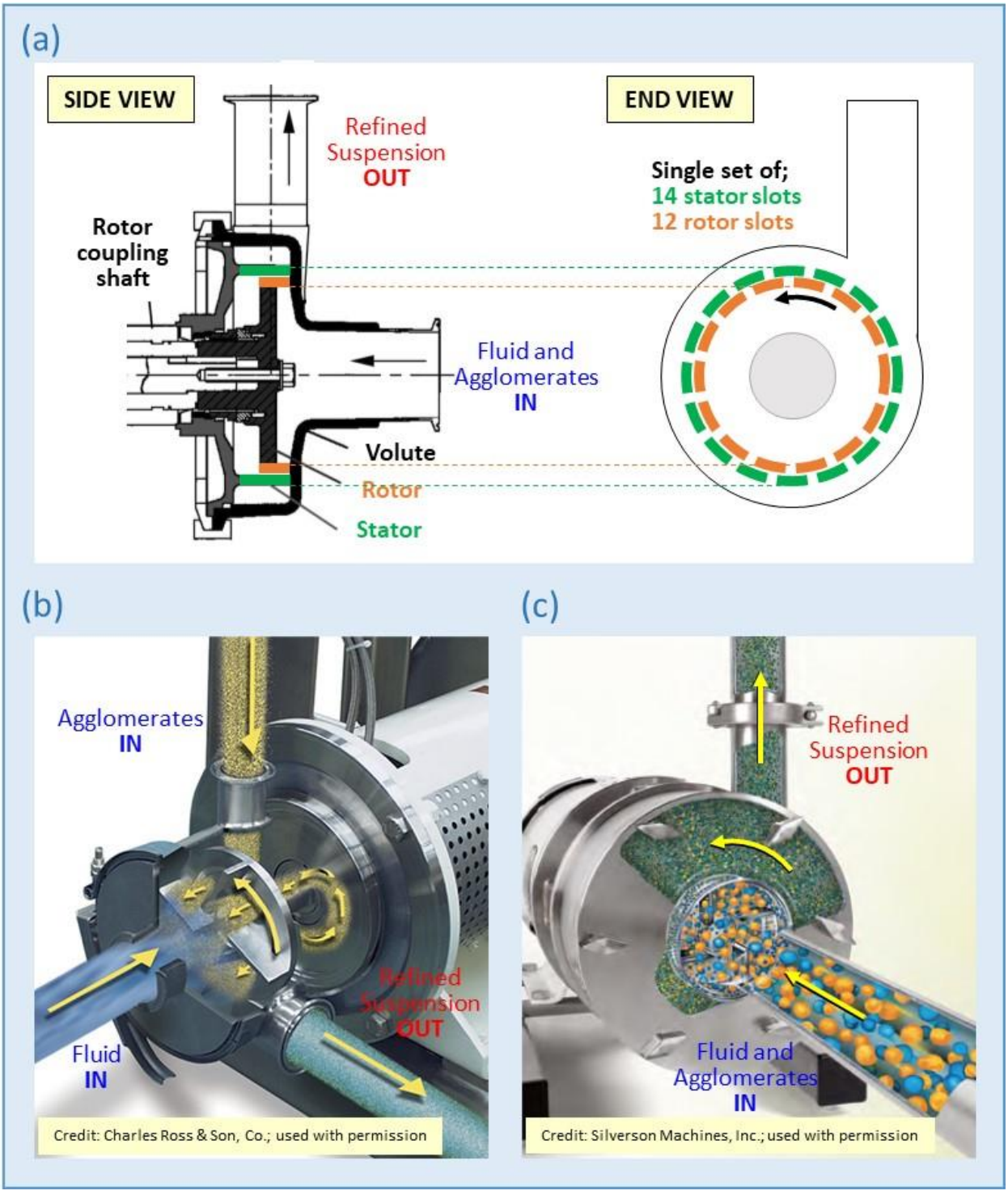

Figure 6. High shear force agitation; (a) typical rotor-stator configuration [ref. 17]. Commercial in-line devices for processing nanoscale dispersions; (b) separate fluid and agglomerate feed [ref. 21]; (b) combined fluid and agglomerate feed [ref. 22].

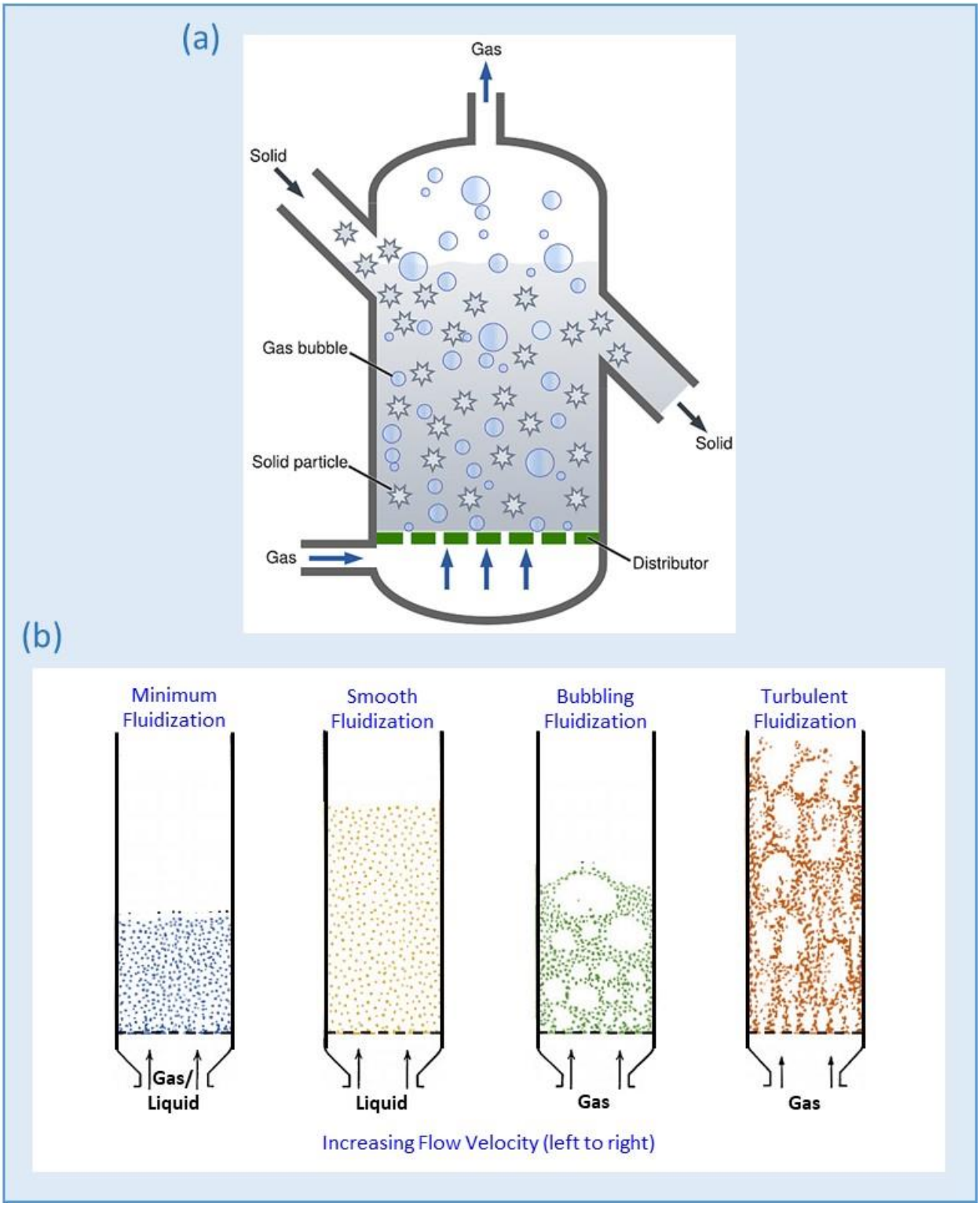

Figure 7. Fluidized bed treatment of agglomerates; (a) goal is homogeneous expansion of particle/fluid mixture by aeration [ref. 24]; (b) processing parameters, such as working fluid and flow velocity, govern cluster size exiting the reactor [ref. 25].

Mechanically enhanced fluidization has proved to be an efficient way to disperse and process nanopowders, accepting that such processing tends to be solvent-intensive [ref. 27]. Although incapable of creating a suspension of individual nanoparticles, the approach is able to generate very fine and dilute agglomerates. Low energy, vibratory fluidized beds reduce the agglomerate size into the ≈ 100 μm range. Acoustic fluidized beds further reduce the agglomerate size into the ≈ 10 μm range [ref. 28]. Augmented with high energy supercritical fluid processors, the agglomerate size can even be reduced into the ≈ 1 μm range [ref. 29]. Methods outlined in a patent suggest effective fluidization of nanoagglomerates using a fluidized bed in conjunction with an applied external field, such as sonication or centrifugation [ref. 30].

1.2.3. Sonication

The use of fluidized beds in combination with acoustic vibration is effective at handling very fine particles [ref. 28]. Deagglomeration is caused by inertial cavitation, where the continual formation and implosion of vacuum bubbles creates extreme turbulence in solid-liquid mixtures [ref. 31]. Ultra-sonification represents a logical progression for manipulating nanoscale particulate (figure 8(a)). Ultrasonic vibrators are used commercially in a wide range of physical, chemical, and biological processes to disperse aggregates and agglomerates into uniform suspensions [ref. 32].

High-intensity, low-frequency ultrasound has proved to be the most effective at imparting the necessary dispersive energy to nanoparticle suspensions [ref. 33]. In general, the fragmentation of agglomerates is only temporary unless the energized product can be stabilized thereafter (figure 8(b)). Thus, ultrasonic processing benefits from surfactant additives that reduce inter-particle cohesive forces, promote deagglomeration, and inhibit reagglomeration [ref. 28]. This technique has been successfully applied to the short-term dispersion of CNTs in aqueous solutions containing organic surfactants [ref. 34].

1.2.4. Ultrasonic Nozzle

In contrast with traditional high-velocity nozzles, low-velocity ultrasonic nozzles do not force liquids through a small orifice using high pressure (figure 9(a)). Liquid is fed through the center of a nozzle with a relatively large orifice and is atomized solely due to ultrasonic excitation [ref. 35]. Resonant frequencies cover the 20–180 kHz range and the droplet size, which is inversely proportional to the frequency, is in the range of 10–40 μm. The demonstrated advantages of this approach include damage mitigation and enhanced dispersion of nanotubes (figure 9(b)). Typically categorized as a coatings technology, reproducible thin films of CNTs have already been deposited on non-planar substrates using solvent-intensive, ultrasonic sprayers [ref. 36].

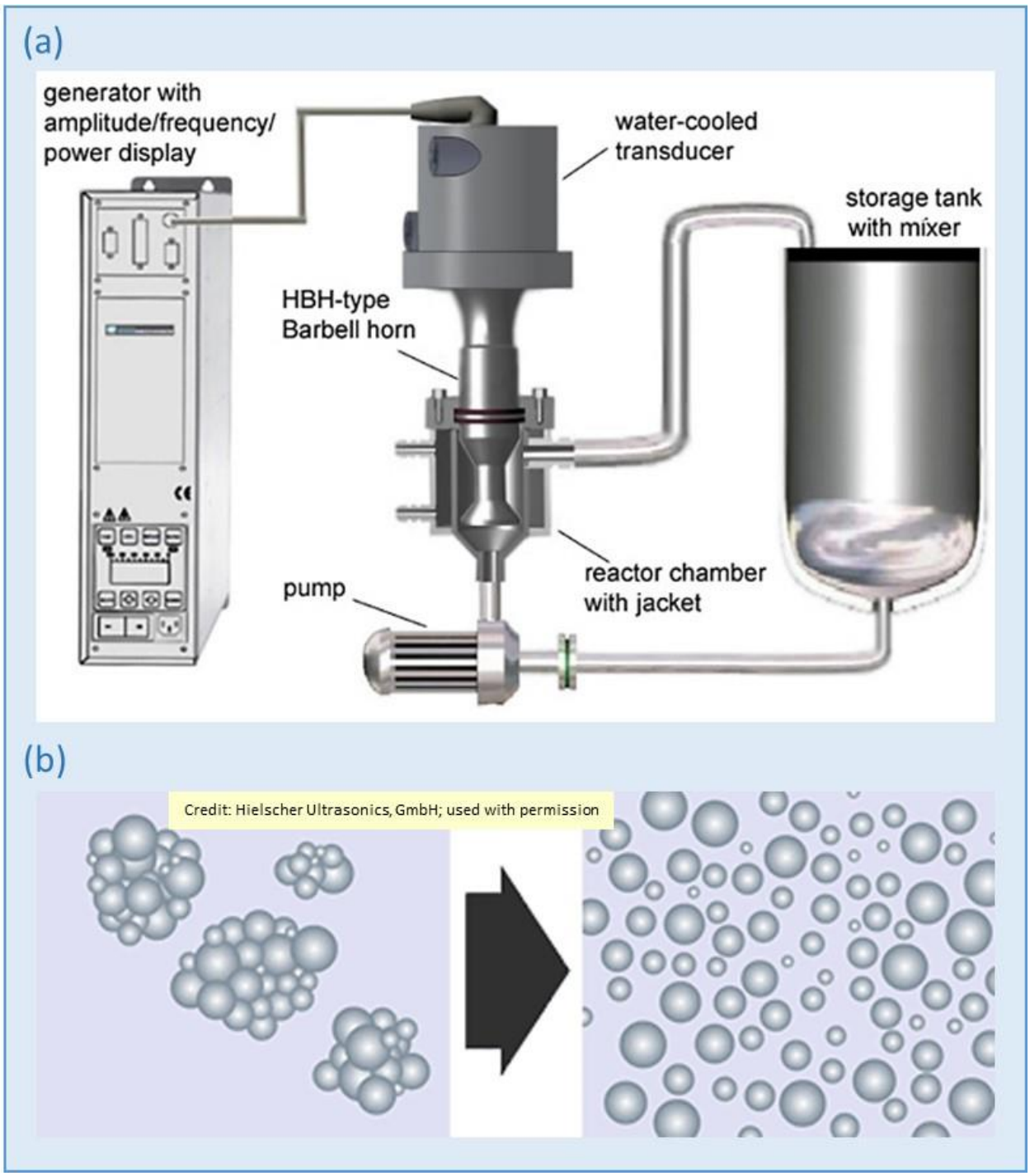

Figure 8. Sonication of particle suspensions using ultrasound; (a) typical equipment in closed-loop configuration [ref. 32]; (b) agglomerates are reduced to clusters, smaller bundles, or individual particles [ref. 33].

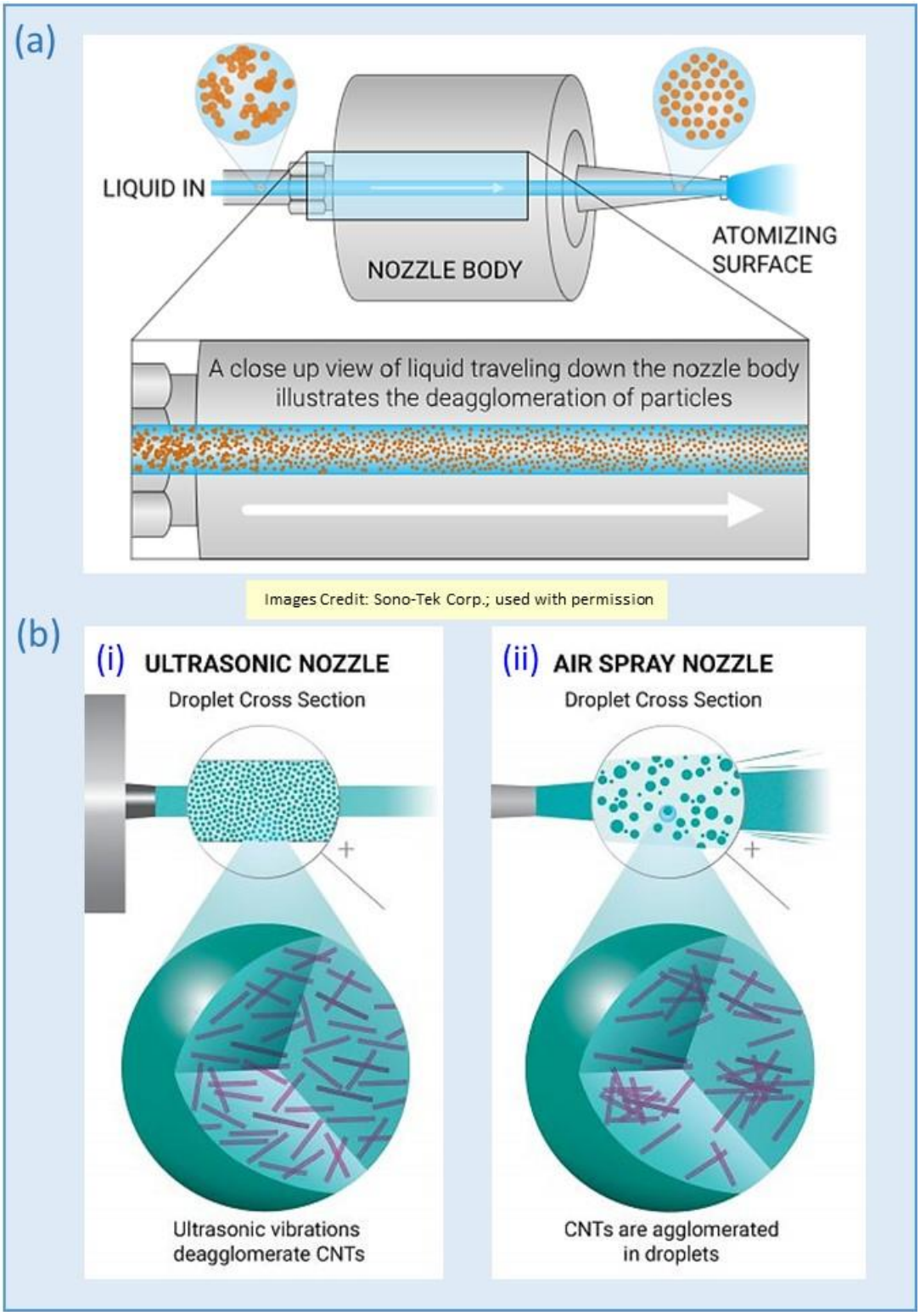

Figure 9. Ultrasonic nozzle; (a) deagglomeration of particle clusters inside nozzle body; (b) benefit of (i) low pressure ultrasound compared with (ii) high pressure air spraying of CNTs [ref. 35].

1.2.5. Supercritical Fluid Processing

The use of fluidized beds in combination with supercritical fluids is effective at handling nanoparticles [ref. 29]. A supercritical fluid (SCF) is any substance at a temperature and pressure above its critical point on the phase diagram where the liquid and gas phase are indistinguishable [ref. 37]. The physical properties of SCFs, such as density, viscosity, and diffusion coefficient, have values that are intermediate between the liquid and gas states. The ability to effuse through a solid like a gas or dissolve a solid like a liquid constitutes the unique characteristic of an SCF. It is noteworthy that the inorganic substances most frequently employed as SCFs include carbon dioxide, nitrous oxide, ammonia, and water [ref. 38]. Both carbon dioxide- and water-based SCFs are prevalent in commercial applications, such as decaffeination of coffee or fractionation of crude oil.

Two of the more common SCF processing techniques are illustrated in figure 10. The methods are often referred to as "rapid expansion of supercritical solutions" (RESS) [ref. 39], and "rapid expansion from supercritical to aqueous solutions" (RESAS) [ref. 40]. The mode of operation when expanding an SCF relies on particle solubility: deagglomeration of insoluble particles from a suspension, and particle synthesis from a supersaturated solution [ref. 41]. Depending on the way the end product is captured, RESS may be considered a dry method (figure 10(a)), and RESAS is classified as a wet method (figure 10(b)). A major reason for considering SCF processors for deagglomeration is that ultrasound-assisted dispersion of CNTs has been achieved while minimizing damage [refs. 42 and 43]. Both techniques operate effectively with carbon dioxide or water as the working fluid, which represents a significant benefit when BNNT processing can be confined to inorganic solutions [ref. 7].

RESS is used commercially to produce fine particles for the food, cosmetics, and pharmaceutical industries [ref. 39]. In general, organic material is dissolved in supercritical carbon dioxide and then the solution is rapidly vented through an expansion nozzle into air. Deagglomeration of insoluble CNTs by RESS has already been investigated with some success. The entangled product was agitated with carbon dioxide under supercritical conditions and then expanded through a fine capillary nozzle. In one example, it was determined that increasing the pressure and/or decreasing the orifice diameter enhanced fragmentation of the agglomerates [ref. 41]. In another example, the median agglomerate diameter of commercial products was reduced by approximately an order of magnitude without sacrificing the AR of the CNTs [ref. 44].

RESAS is a variation of the RESS process in that the SCF is expanded into a liquid, rather than a gas [ref. 40]. An advantage of this technique is the ability to more readily stabilize suspensions of deagglomerated particles. The use of aqueous solutions that contain surfactants or dispersants facilitates subsequent handling and application [ref. 45]. Commercially, the technique is most widely used in drug manufacture, where compound ingestability can be enhanced by synthesizing nanoparticles [ref. 46]. The approach has also been applied to the fabrication of CNT-reinforced PMCs, leading to improved distribution within the liquid matrix precursor [ref. 47].

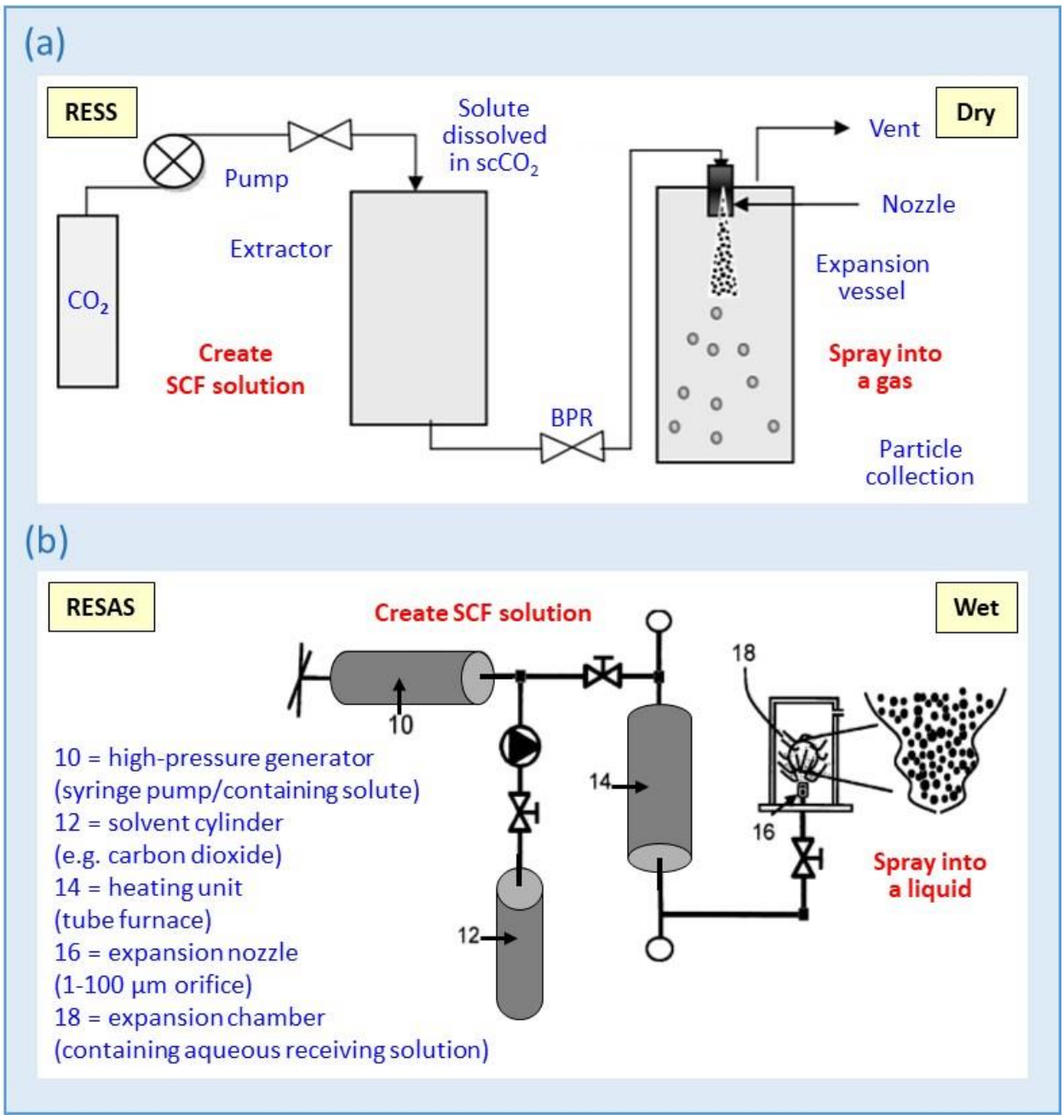

Figure 10. Customary supercritical fluid (SCF) processing techniques: (a) rapid expansion of supercritical solutions (RESS) - spraying into a gas [ref. 39]; (b) rapid expansion from supercritical to aqueous solutions (RESAS) - spraying into a liquid [ref. 40].

1.3. Purification Devices

Purification involves removal of by-products from the reactor effluent (during synthesis) or an impinging stream (post-synthesis). In essence, the process comprises isolation of BNNTs via mass- or size-based fractionation on a coarse scale. Cyclonic separation serves this purpose well and is available in a variety of basic forms. The technology is applicable to continuous or batch processing and is compatible with dry, moist, or wet operating conditions.

1.3.1. Tribocyclone Separator

Tribocyclones, also known as triboelectric cyclones or chargers, rely on surface charging of insulating particles by frictional contact (figure 11). The technology is applied commercially in the recycling industry for separating various types of plastics based on differential charging behavior [ref. 48]. In one manifestation, particulated mixtures are triboelectrically charged in a cyclone that feeds an electrostatic separator (figure 11(a)) [ref. 49]. Particle deflection within the electric field is governed by the polarity and magnitude of surface charge assumed by individual polymers. The resulting spectrum of trajectories allows for composition-based fractionation into a linear array of collecting bins or trays.

In another manifestation, granular mixtures are diverted using a vertical triboelectric separator (figure 11(b)) [ref. 50]. Most efficient when all particles are composed of a single material, the polarity and magnitude of the triboelectric charge is influenced by particle size or morphology. Generally, smaller particles charge negatively, and larger particles charge positively for a given size distribution [ref. 51]. The deviation of particle shape from spherical strongly influences tribocharging behavior via the contact mode, the mean contact area, and the contact duration [ref. 52]. It may be possible to exploit these phenomena for either size- or shape-based fractionation purposes.

1.3.2. Electrocyclone Separator

Conventional gas cyclones rely on inertial separation and are most effective for collecting mass quantities of particles > 1 μm in diameter. Electrocyclones were developed to filter particles in the submicron range by augmenting the separation process with an electric field [ref. 53]. The insertion of an axial electrode charges particles by the corona effect, and the finer particles are attracted to the grounded cyclone walls by electrostatic forces (figure 12(a)(i)). Particles in the size range 10–30 nm form micron-sized aggregates that precipitate on the walls for subsequent removal [refs. 54 and 55].

Often referred to as electrostatic cyclones, such devices are compatible with high throughputs, elevated temperatures, and harsh operating environments. Commercial application includes improving the efficiency of particulate control in the aerosol industry [ref. 56]. An innovative design, figure 12(a)(ii), demonstrates that electrocyclones can also operate under wet conditions for collecting nanoparticles [ref. 57]. A recent patent teaches in-line separation of CNTs from gaseous reactor effluent during commercial production with electrocyclones as an option (figure 12(b)) [ref. 3].

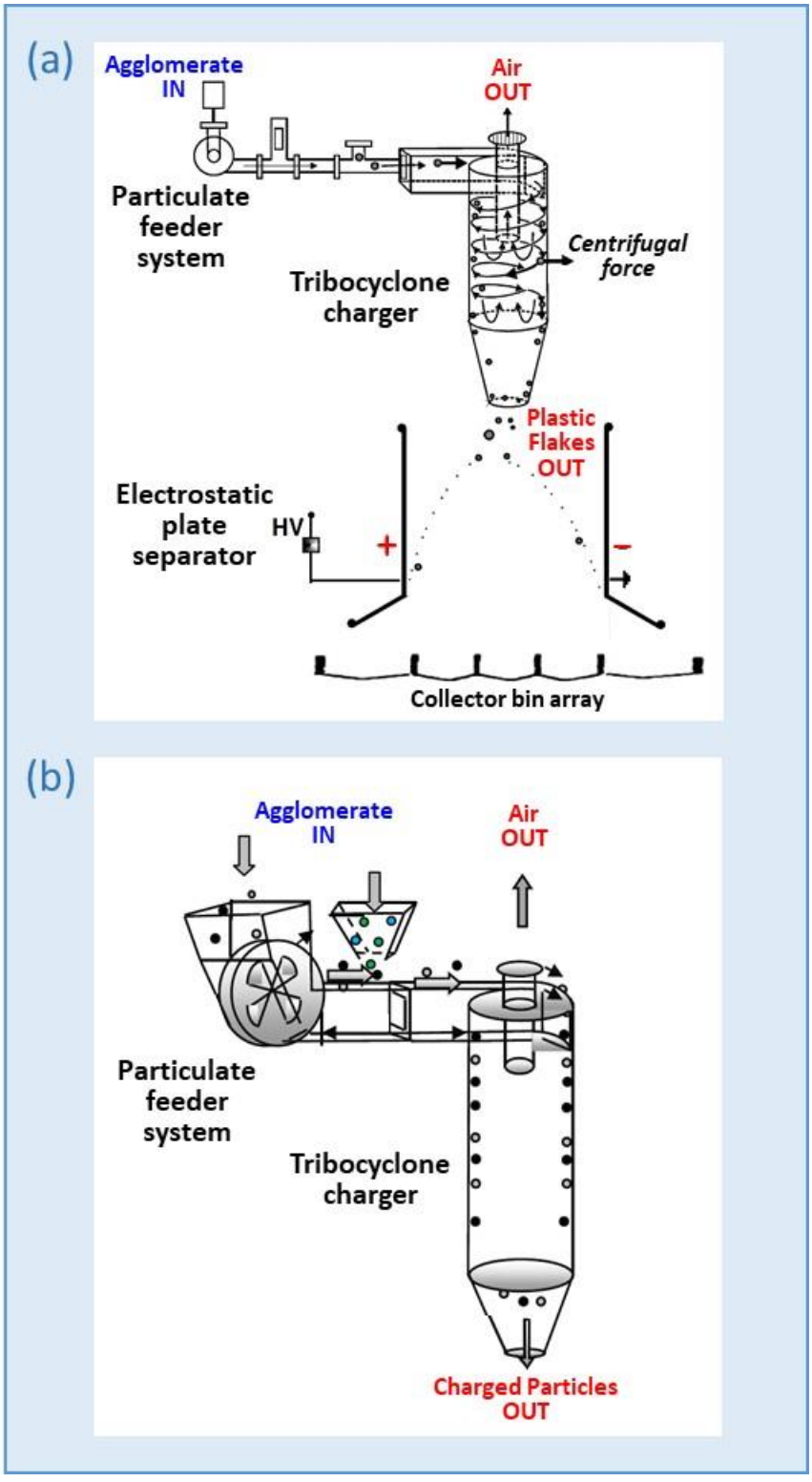

Figure 11. Common tribocyclone configurations; (a) triboelectric charger feeding electrostatic separator for composition-based fractionation [ref. 49]; (b) triboelectric division of non-conductive particles based on size/morphology [ref. 50].

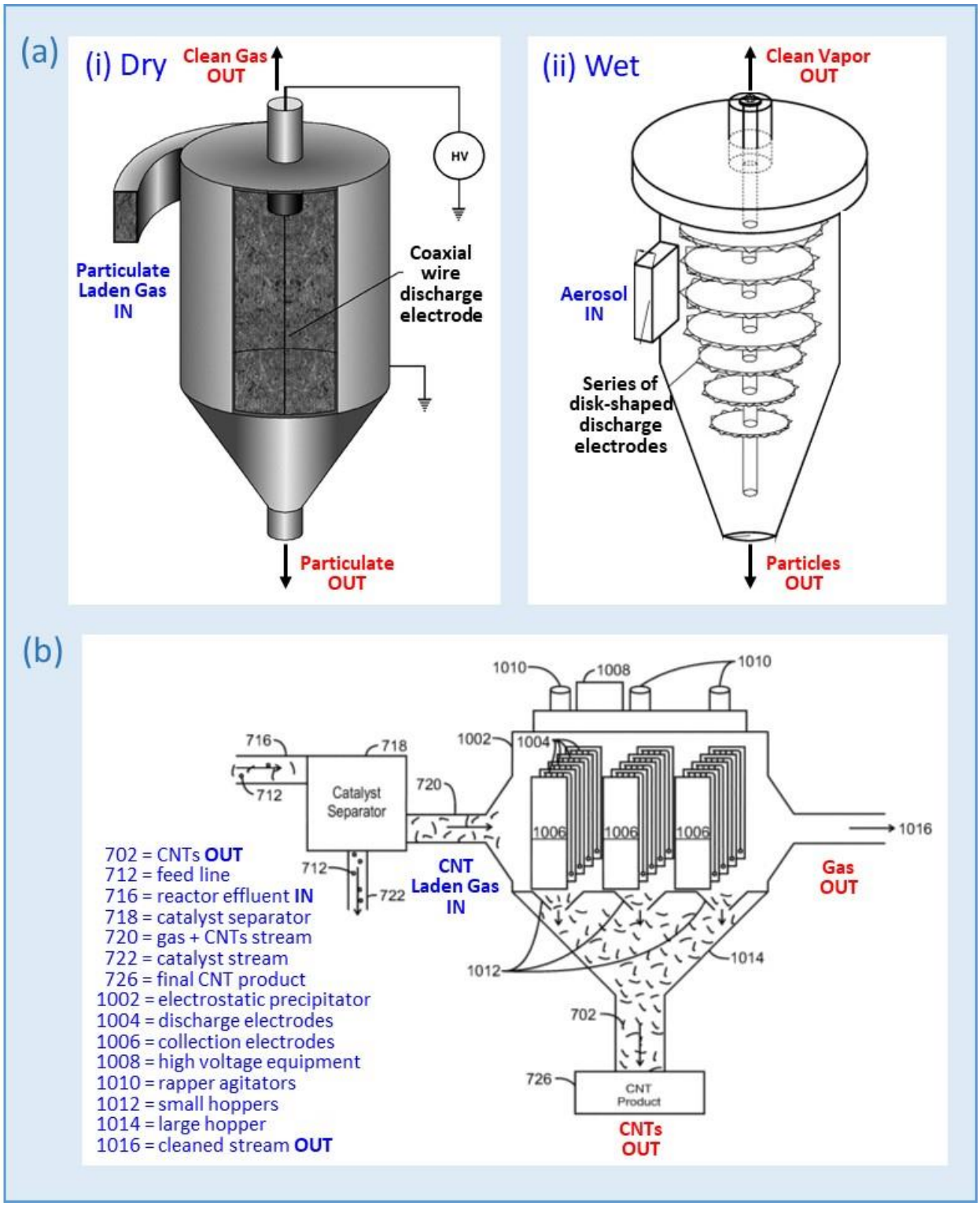

Figure 12. Typical electrocyclone configurations; (a)(i) dry operations - axial wire electrode [ref. 55]; (a)(ii) wet operations - series of disk electrodes [ref. 57]; (b) moist operations - option for nanotube separation system during synthesis [ref. 3].

1.3.3. Hydrocyclone Separator

Hydrocyclones use fluid pressure to generate centrifugal force and spiral flow to extract particles from a liquid medium. The density of the working fluid must be greater than the density of the particles for effective separation [ref. 58]. Customarily mounted vertically, the configuration comprises an upper, cylindrical chamber connected to a lower, conical body (figure 13(a)) [ref. 59]. Fluid enters the upper chamber tangentially creating vortices in the lower body : an outer helical flow (descending) and an inner axial flow (ascending).

The cyclonic action divides the fluid between two outlets, based on suspended particle size. Larger particles exit at the bottom of the cone, termed "underflow" discharge. The smaller particles exit through an axial pipe projecting into the top of the chamber, termed "overflow" discharge. The geometry of the device determines the cut-off in particle size between the overflow and underflow [ref. 60]. On this basis, an arrangement of devices with varying geometries is capable of size-based separation of particulate. Details of an older patent teach that a series of hydrocyclones can be tangentially staged to produce multiple fractions in unison (figure 13(b)) [ref. 61].

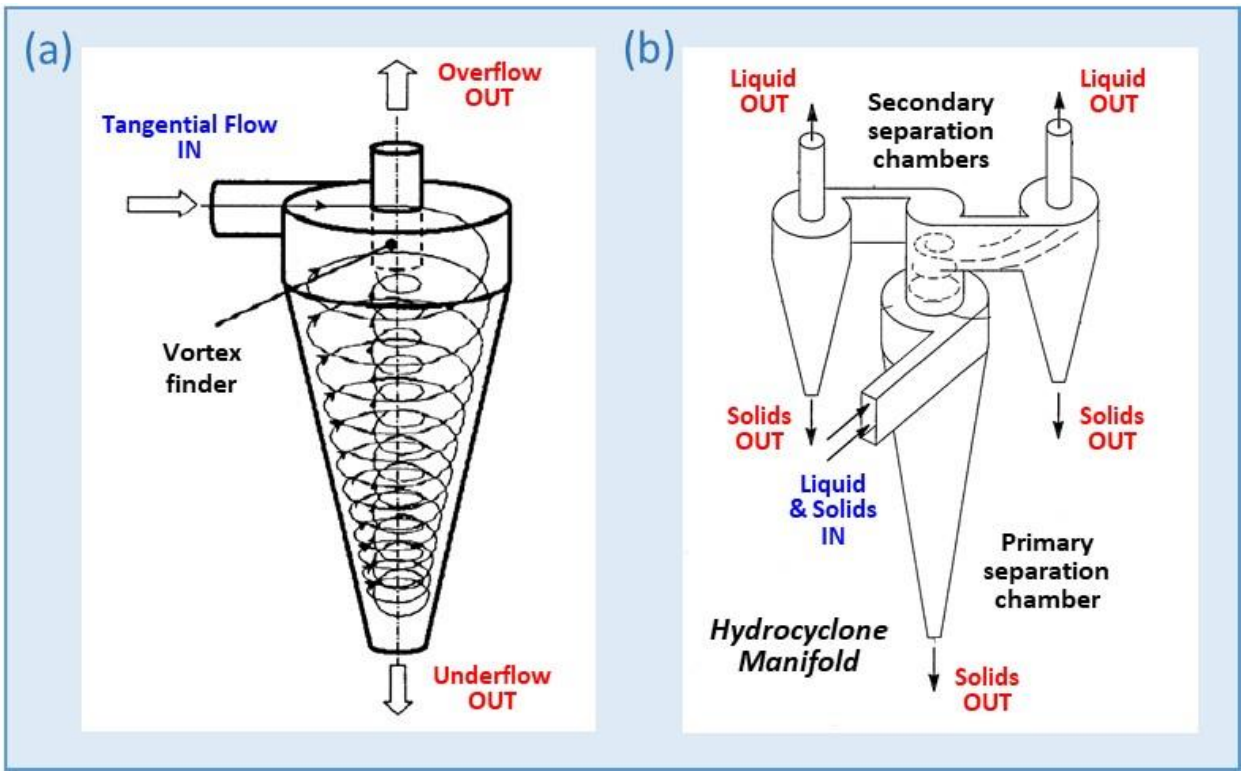

Figure 13. Hydrocyclone configurations; (a) typical unit with tangential input and twin axial outputs for overflow and underflow [ref. 59; (b) staging of multiple units to yield a variety of particle fractions [ref. 61].

The technology is most commonly applied in the mining industry and has found a niche in coal liquefaction processes [ref. 62]. Typically, hydrocyclones are effective at solid-liquid separation for particle diameters terminating in the 5–10 µm range [ref. 63]. The smaller the diameter, the higher the centrifugal force, and the higher the efficiency of small particulate isolation. Highly elongated cone designs have been developed that extend performance to particle sizes below 5

μm. A recent patent related to commercial production teaches in-line separation of CNTs from a water stream with a hydrocyclone device as an option [ref. 64].

1.4. Fractionation Devices

Fractionation involves separating BNNTs into narrow lots based on length or morphology. The continuous or batch process comprises division of BNNTs via shape-based fractionation on a fine scale. Electrophoretic, acoustophoretic, or electrostatic separation techniques offer the most potential and operate in a range of environments.

1.4.1. Electrophoresis/Dielectrophoresis

The technique of electrophoresis/dielectrophoresis fractionates particles by relative mobility through a working fluid in response to a transverse electric field [ref. 65]. Typically, particles are suspended in a wet solution (liquid phase), but suspension in a dry gas or moist vapor can also be employed (gas phase). The more common liquid phase electrophoresis employs direct current to create a uniform electric field across a flowing suspension (figure 14(a)) [ref. 66]. Separation occurs because charged particles migrate at different rates, dependent on mass, size, and/or shape. It has been demonstrated that electrophoresis separates < 50 nm particles by size and charge with 97% collection efficiency [ref. 67].

In contrast, liquid phase dielectrophoresis uses alternating current to create a non-uniform electric field across a flowing suspension (figure 14(b)) [ref. 68]. Separation occurs because polarized particles have differing mobilities that depend on electronic properties. It has been demonstrated that dielectrophoresis separates 30–60 nm particles by size and polarizability with 85–100 percent collection efficiency [ref. 67]. Traditionally used to isolate analytical batches of nanoparticles by size, the separation principle may be applied to a continuous processing scenario.

Application of the technology to sorting nanotubes is most pertinent to this survey. Liquid phase electrophoresis has successfully been employed to separate CNTs by length and diameter simultaneously [refs. 69 and 70]. It has been established that ultrasonic agitation enhanced separation and facilitated scale-up to larger quantities. An associated technology known as "field flow fractionation" relies on the influence of a transverse electric field on fluid flowing through a narrow channel [ref. 71]. The fluid velocity assumes a parabolic profile under laminar flow conditions, being highest at the center and lowest at the walls. This technique has been exploited to extract CNTs from a suspension, while sorting small quantities by size [ref. 72], length [ref. 73], or shape [ref. 74].

In addition, gas phase electrophoresis has been deployed during synthesis for length classification of diameter-controlled CNTs suspended in an aerosol (figure 14(c)) [ref. 75]. Electrostatic mobility separators arranged in-tandem determine the diameter, then the length, of pre-charged product. The in-flight method can be deployed to control the diameter and length of CNTs during a catalytic growth process, or to determine the AR distribution of CNTs produced by some arbitrary process. The philosophy has merit and could be adopted for length-based fractionation of uniform diameter BNNTs. However, the narrow size distribution and very low throughput challenge the practicality of scale-up to mass production of reinforcing agents.

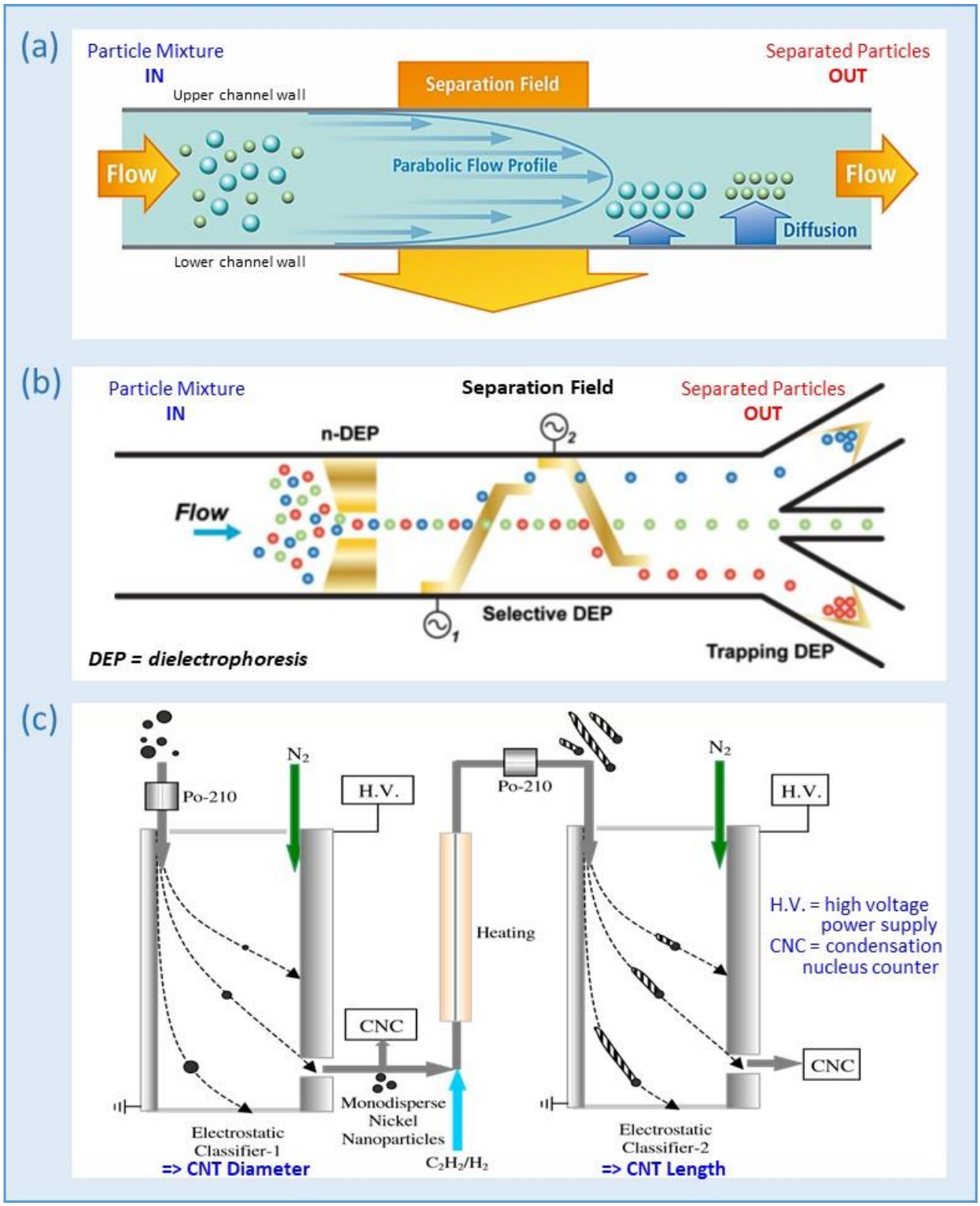

Figure 14. Principles of size-based electrical fractionation of nanoparticles; (a) liquid phase - DC electrophoresis [ref. 66]; (b) liquid phase - AC dielectrophoresis [ref. 68]; (c) gas phase - electrophoretic classification of CNTs by size during synthesis [ref. 75].

1.4.2. Acoustophoresis

Acoustophoretic separation also resides within the realm of free- or field-flow fractionation processes [ref. 76]. In contrast with the electric fields used in electrophoresis, acoustophoresis employs sound waves for the differential extraction of particles from a carrier fluid. It has been demonstrated that acoustophoresis separates < 200 nm particles by size and density with > 90% collection efficiency [ref. 67]. Both are classified as analytical techniques for quantifying particle distributions owing to the relatively low throughput for other applications. However, these techniques are included in this review because the principles involved may be exploited to enhance other processes compatible with handling mass quantities.

Using acoustophoretic techniques, the carrier fluid can be either a gas or a liquid. Gas phase acoustophoresis is considered to be an emerging technology. An ultrasonic standing wave applied to laminar flow, with a parabolic velocity pattern, forces the largest to the center and the smallest to the walls of a resonator channel (figure 15(a)) [ref. 77]. The acoustic power required to manipulate particles within gas is an order of magnitude higher than with liquid as the transport medium. Nevertheless, efficient size-based fractionation of 30–600 nm diameter aerosol particles suspended in a continuous air flow has been accomplished [ref. 78].

Liquid phase acoustophoresis is the established technology that has been adopted in many microfluidic systems. Mixed particle suspensions are channeled into dynamic fractions that are separated into multiple outlets by size and/or density (figure 15(b)) [ref. 79]. Free-flow fractionation has been employed to separate micron-sized particles by creating laminar flow in a tube and subjecting to an acoustic field. Customarily, particle size separation involves using acoustic valving to divert the inlet flow into two outlet flows. However, multiple fractions are obtainable when such binary sorting devices are arranged in a tree configuration (figure 15(c)) [ref. 80].

This concept is applicable to any particle-sorting device and might be adaptable to shape-based fractionation of BNNTs on a highly refined scale. A NASA patent teaches separation of particles from a liquid medium via a batch process, where acoustic wave frequency governs the particle size extracted [ref. 81]. More recently, standing waves have been employed for size-based fractionation of nanoparticles in a continuous flow [ref. 82]. Several patents related to water purification teach methods for fast, high-volume separation of ultrafine particles from fluid suspensions [ref. 83].

1.4.3. Electrostatic Separator

Electrostatic separation technology is applied under dry, moist, or wet operating conditions, and equipment configuration is material-dependent [ref. 84]. The various devices rely on an applied electric field to isolate and collect particles from a suspension and can be categorized by function. Electrostatic *precipitators* are traditionally employed for emission control and are normally of the parallel plate or wire-in-tube variety [ref. 85]. This type is used extensively by many commercial entities for collecting mass quantities of sub-micron and irregularly shaped particles [ref. 10]. In contrast, electrostatic *separators* are primarily employed for product recovery and are frequently of the rotating drum variety for continuous handling of large volumes [ref. 86]. Particle fractionation is normally restricted to separation of conductors from semi-conductors and/or non-conductors (dielectrics) [ref. 87].

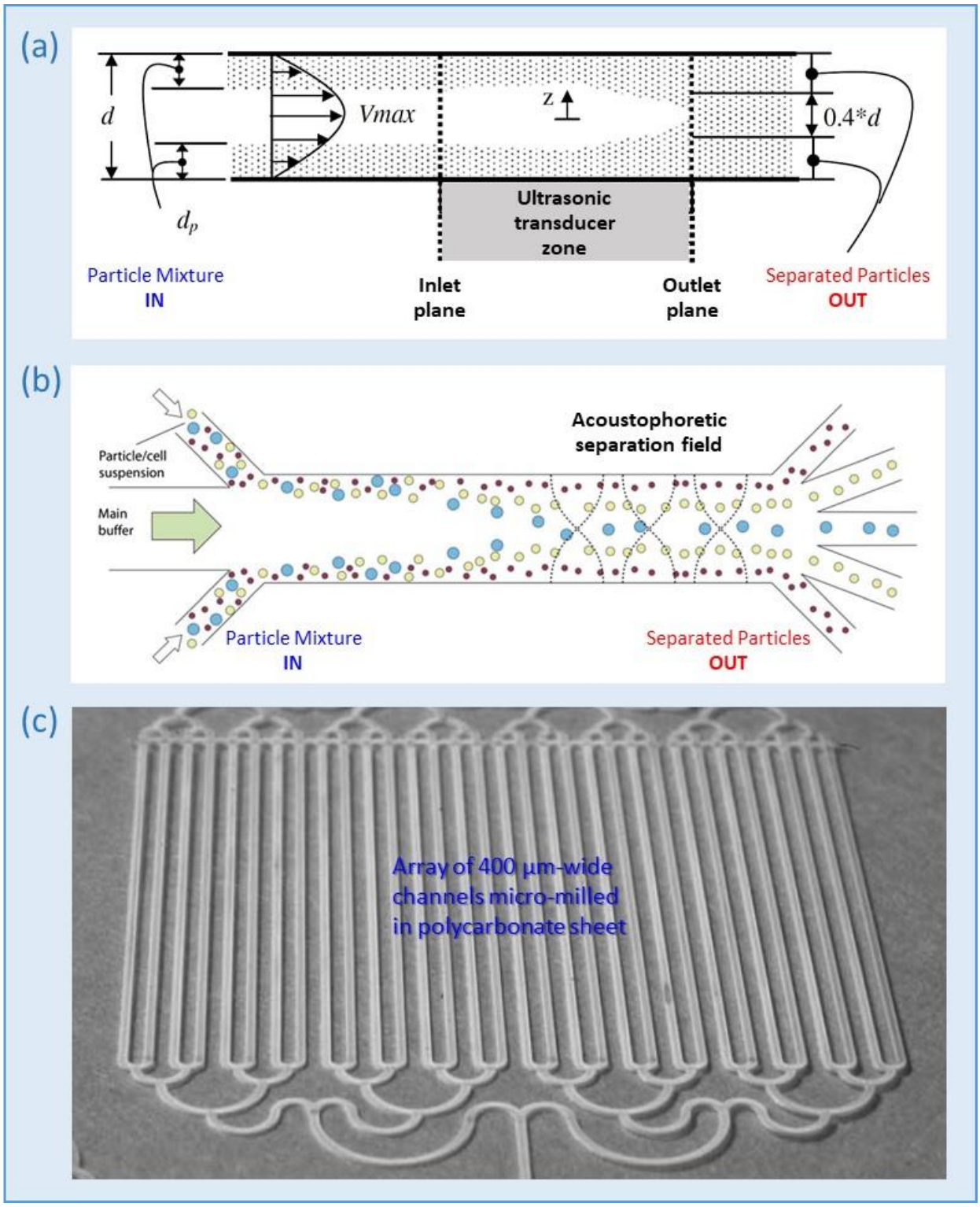

Figure 15. Acoustophoresis; (a) gas phase - using an ultrasonic standing wave [ref. 77]; (b) liquid phase - separation of mixed suspensions [ref. 79]; (c) "tree" configuration for generating multiple fractions simultaneously [ref. 80].

Among the many electrostatic separators, the high-tension, rotating drum configuration appears best suited to mass quantities [ref. 88]. The technique is widely used in the minerals industry for handling large volumes in either a continuous or a batch process [ref. 89]. Most non-metallic materials exhibit conduction when the potential difference is sufficient, therefore particle separation relies on differential conductivity [ref. 90]. All the particle types entering the field are charged and adhere to the rotating drum as a consequence. The junctures at which the different species are ejected from the surface depend on both the size of the initial charge and the rate of charge decay [ref. 91]. These mechanisms depend not only on particle size, but more importantly on particle morphology and form the basis for shape-based fractionation.

The two basic types of rotating drum separators operate on electrophoresis or dielectrophoresis principles under dry/moist or wet conditions, respectively (figure 16) [refs. 92 and 93]. Electrophoretic separation involves charged particles and usually exploits differential charging of conductive materials [ref. 89]. The process employs a uniform or non-uniform electric field induced by direct current and is conducted exclusively in gas or vapor phase. There is also the choice of using either a bare metallic (conducting) drum or an insulative coated (semi-conducting) drum. Particle mixtures can be charged in three distinct ways: corona charging, induction charging, or tribocharging. Corona charging is by far the most common method used in roll-type electrostatic separators (figure 16(a)) [ref. 92]. The practice involves a point source under high tension that discharges ions which bombard the incoming particles. Customarily, the corona source and the grounded metal cylinder constitute the positive and negative electrodes containing the divergent electric field.

In contrast, dielectrophoretic separation involves uncharged particles and typically exploits differential polarization of non-conductive materials [ref. 89]. The operation employs a non-uniform electric field induced by direct or alternating current (DC or AC) and is conducted in the liquid phase. The process uses a drum with fine wires placed along its surface, parallel to its axis (figure 16(b)) [ref. 93]. A screen electrode is submerged in a dielectric fluid beneath the drum, and an AC potential is placed across the electrode and drum assembly. Particles of a higher dielectric constant are fed onto and attracted to the region of high electric field gradient (the wires) on the drum's surface. Lower dielectric constant material is repelled to a region of low field gradient by an intermediate dielectric fluid and falls through the screen electrode [ref. 87]. Customarily, liquid phase separation by a wet, drum-type separator employs an organic dielectric fluid, but deionized water may be a workable option [refs. 94, 95, and 96].

A sub-category of electrophoretic separation using ion bombardment, rotating drum separators is known as electrostatic shape separation. The approach relies on controlled charging techniques to separate materials based on the particle's shape and density without consideration of the inherent conductivities of the constituents [ref. 89]. The surface area to mass ratio is much higher for flat particles than spherical particles making the technique a charge-selective rather than a size-selective process. The isolation of particles with a specific morphology can be achieved via consideration of the "flatness" coefficient. This comprises the length-to-thickness ratio, and the higher the coefficient, the flatter the particulate [ref. 97].

Unlike conventional methods in which separation is based on conductivity, separating by morphology requires dedicated roll construction. Traditional corona field separation uses a grounded metallic roll electrode, but an alternate method uses a metallic roll that is covered with an insulating overlayer (figure 17(a)) [ref. 98]. The patent teaches a conductive steel roll (2)

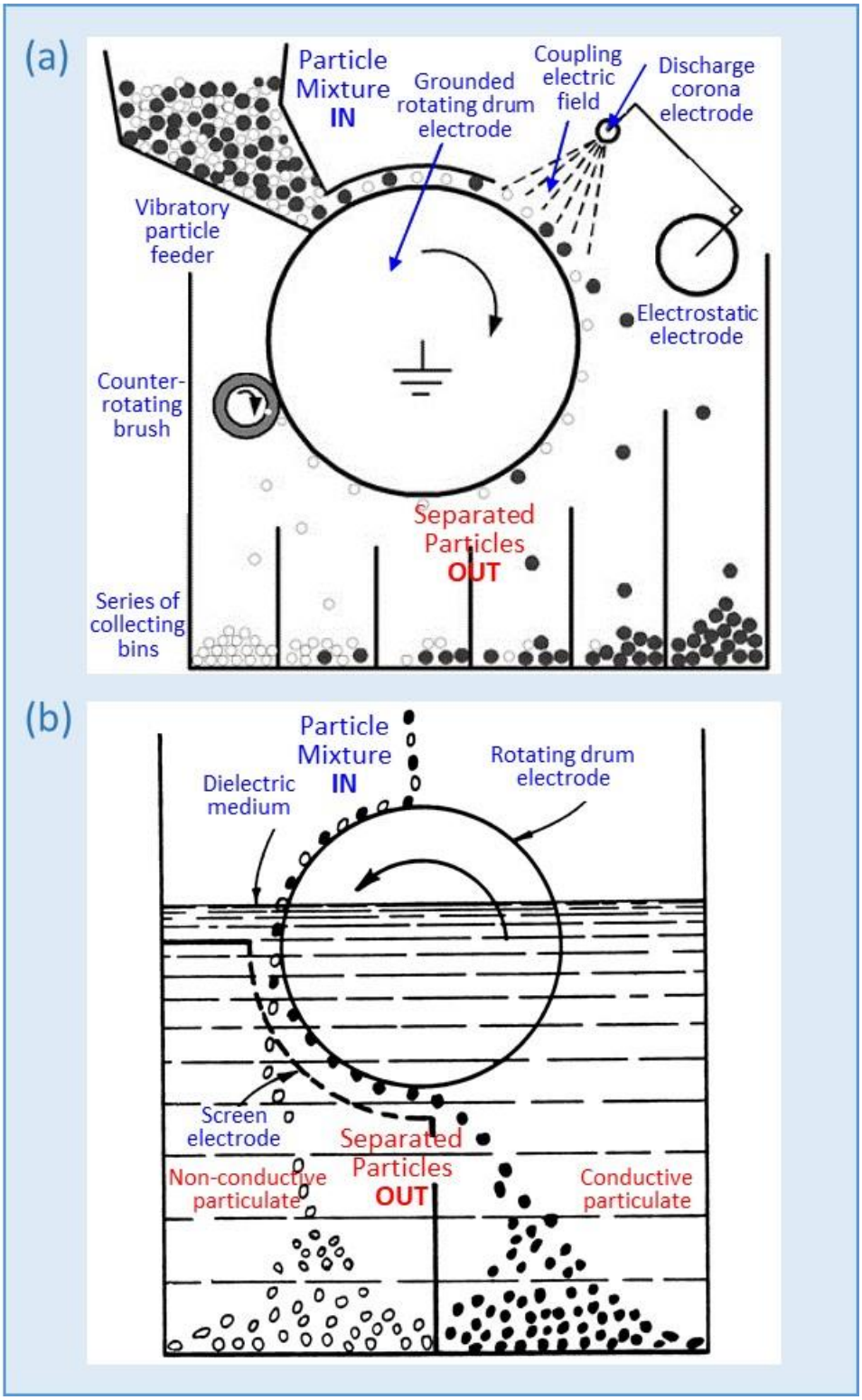

Figure 16. Rotating drum-type electrostatic separators operating in dry or wet conditions; (a) gas phase - electrophoretic separation [ref. 92]; (b) liquid phase - dielectrophoretic separation [ref. 93].

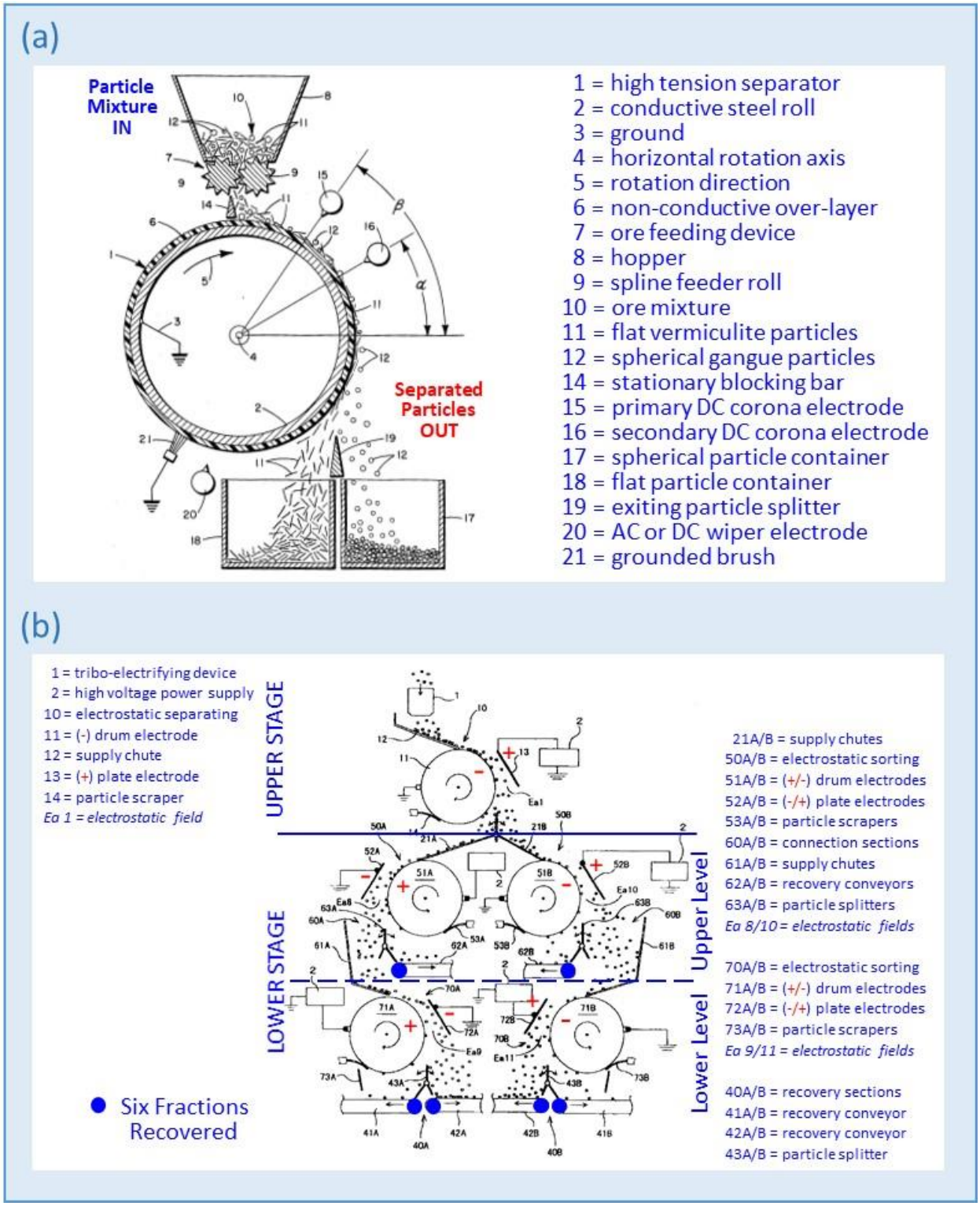

Figure 17. High tension/corona discharge, rotating drum separators: (a) electrostatic shape separation [ref. 98]; (b) a sequence of units for creating multiple fractions [ref. 99].

with a non-conductive polymeric or ceramic coating (1) that is 1.25 - 4 mm thick. The arrangement comprises two DC corona discharge electrodes of the same polarity to attract the particles to the rotating drum (15 and 16) and a DC corona electrode of opposite polarity to eject selective particles (20). Another patent teaches the arrangement of drum-type separators for generating multiple fractions in a sequential process (figure 17(b)) [ref. 99].

All of these various techniques are routinely engaged for the sorting of dissimilar materials by electrical properties, however the focus of this survey is sorting of the same material by particle dimensions. Although a less common application, some of the techniques are capable of classification by size and/or morphology. The underlying principle of electrostatic separation is that an applied electric field charges conducting particles and polarizes non-conducting particles [ref. 87]. The diameter of spheroids and the length of ellipsoids govern the total charge imparted on conductive materials and the net charge imparted on non-conductive materials [ref. 89]. Both approaches have proven effective for separation of sub-micron particles, but the ability of either technique to classify nanotubes remains under development [ref. 100]. One issue that remains unresolved concerns whether nanotubes can be separated individually, or rather as bundles that require further disentanglement for length fractionation purposes.

1.5. Collection Devices

The performance of nanotube-containing structural materials will be governed not only by reinforcement morphology, but also by the integrity of the reinforcing agent/matrix interfaces. , Dependent on thermal history, reactions during processing of Al and Ti alloys have resulted in carbide formation in CNT-MMCs [refs. 101 and 102], or (to a lesser extent) nitride and boride formation in BNNT-MMCs [refs. 103 and 104]. Even though serendipitous benefits to nanotube/matrix bonding have been noted, precipitation of these compounds must be minimized. Such interfacial phases tend to be brittle and act as mechanical defects. In addition, the nanotubes are partially consumed and no longer pristine, thereby reducing load-bearing capability [ref. 105]. Interfaces in BNNT-MMCs will be further compromised by carbides, and hydrocarbons are very difficult to eliminate from BNNT products once introduced [ref. 7]. It is also known that carbon contamination deteriorates both the physical and mechanical properties of BNNTs [ref. 106]. Although organic fluids may be used for CNT transport without penalty, focusing research and development on inorganic media for BNNT storage seems prudent.

Commercial lots of fractionated BNNTs for discontinuously reinforced composites must be available in a highly usable product form, such as paintable liquid or spreadable paste. Customarily, the uniform dispersion of ultrafine particles in a working fluid can be divided into three, distinct processes: wetting, deagglomeration, and stabilization [ref. 107]. The latter stage is critical in the scalable production of homogeneous suspensions that are compatible with easy storage, transport, and application. Re-agglomeration of BNNTs following separation into fractions by AR is inevitable in the absence of a stabilizing storage medium. Retention of a stable mixture requires balancing the attractive and repulsive forces between particles often through the addition of surface modifying agents such as dispersants or surfactants [ref. 108].

Significant progress has been made at NASA-LaRC towards creating stable suspensions of BNNTs in a wide variety of inorganic fluids [ref. 109]. The prime objective was a uniform dispersion without sonication or functionalization, such that the high ARs and chemical structure

responsible for exceptional properties were preserved. Candidate solvent or solvent pairs for effective BNNT separation were evaluated by exploiting the well-known Hansen solubility parameters (HSP) [ref. 110]. The concept proved to be a practical and powerful way to understand issues of solubility, dispersion, diffusion, and chromatography. This methodology is much more potent than using nebulous solvent characteristics, such as polar, non-polar, hydrophilic, or hydrophobic terminology. The guideline for determining relative solubility of "like dissolves like" is replaced by the differential in HSP between the solid and solute. It was concluded that the probability of obtaining a uniform dispersion is highest when the HSP of a solvent match those of the BNNTs.

Traditionally, solubility theory has been utilized to determine solvent mixtures for dispersing single-walled CNTs [ref. 111] and graphene [ref. 112]. Co-solvents have also been investigated to enhance the solubility of CNTs compared to a single solvent [ref. 113]. Early LaRC work attempted to rank individual solvents by relative dispersion strength to estimate a solubility/dispersion potential, since the HSP of BNNTs were not known. Highly polar, aprotic solvents were identified as the most efficient at dispersing bulk quantities of BNNTs without sonication. Development of effective co-solvents involved mixing of these solvents with protic solvents that reside outside the BNNT solubility region. Specific combinations included dimethylformamide, dimethlysulfoxide, or N-methylformamide mixed with water, methanol, or isopropyl alcohol in proportions ranging from 80:20 to 50:50. Recently, the HSP of purified BNNTs have been determined via sedimentation tests and ranked by relative settling time in different solvents [ref. 114].

Inorganic fluids are recognized as the preferred medium for collection of fractionated BNNT products. Organic fluids are typically defined as having carbon and hydrogen and at least one C-H bond, hence discussion will focus on liquids without those components. Some common inorganic fluids that meet that criterion include water, ammonia, hydrogen fluoride, carbon tetrachloride, sulfuric acid, hydrogen cyanide, and hydrazine. Equally important, a non-hazardous fluid that is liquid at room temperature represents a wise choice for ease of use. Water is the obvious candidate as a storage medium because it is an abundant and safe fluid that satisfies the requirements. Thus, optimizing water's ability to stabilize and maintain a fully dispersed BNNT product without using an organic co-solvent becomes the main task. Inorganic surfactants that can modify the HSPs to match those for the optimized organic co-solvents discussed previously offer the most potential for stable suspensions.

Elsewhere, there has been a concentrated effort to modify BNNTs with hydroxyl or amine side groups [ref. 115]. Treatment of BNNTs with hydrogen peroxide (H_2O_2) at high temperatures and pressures resulted in hydroxyl groups bonding to B sites, while NH groups affiliated with N sites. In contrast with pristine BNNTs, which are hydrophobic, the treated BNNTs became water soluble. This indicates that hydrophilic groups had indeed bonded to the nanotube surfaces. Further, it was estimated that the solubility of H_2O_2-treated BNNTs in water exceeded 0.25 g/l after standing for 48 hours.

An alternate method for modifying BNNTs involves treatment with liquid bromine [ref. 116]. This research provides a scalable three-stage purification protocol for raw BNNT material to yield a purity of ~80 wt.%. The initial two stages remove impurities through water solubility and gravimetric separations. The third stage involves treatment with bromine to chemically remove

elemental boron species. This last step was found to functionalize the surface of BNNTs with –OH and $–NH_2$ groups through B-N bond cleavage when excess bromine was used. These groups form hydrogen bonding networks with water, which lead to pH-switchable solubilization of the resulting BNNTs. Stable aqueous solutions are formed around neutral pH, but BNNTs readily precipitate outside of the $4 < pH < 8$ range.

Dispersing BNNTs without functionalization or use of a surfactant has proven to be challenging. Limited success has been achieved by utilizing superacids, such as chlorosulfonic acid (CSA), for CNTs. It has been shown that reversibly protonating the carbon surface with CSA results in dissolution of single- and multi-walled CNTs [refs. 117 and 118]. More recently it has been demonstrated that BNNTs also readily dissolve in CSA as disentangled individual strands at the molecular level [ref. 119]. Analysis of treated BNNT product indicated reversible dissolution, without damaging or modifying the chemical structure.

Considerable research will be required to create a product that can be readily employed in the manufacture of acreage quantities of BNNT-MMCs. Recognizing that the solvent formulations proffered may not fulfill current needs, the methodologies outlined do provide a basis for preparing stable dispersions of large volumes of BNNTs. Ideally, the suspension must contain non-agglomerated, high-AR BNNTs at relatively high concentration in an inorganic solvent. The most widely accepted transport medium will be relatively inexpensive, non-hazardous, and easily purged from the structural material being fabricated.

2. Ranking Candidate Methods

The results of a survey of established technologies compatible with the handling and sorting of BNNT products are summarized in table 2. The best candidate methods are grouped by function, qualitatively graded relative to discriminating criteria, and divided into two categories:

(i) "Particle Characteristics" relevant to BNNTs:

- Nanoscale, i.e., particles with sub-micron dimensions
- Dielectric, i.e., insulative or non-conductive particles
- Aspherical, i.e., irregular or fibrous morphology

(ii) "Particle Sorting Capability" relevant to BNNTs:

- Particle size, i.e., diameter or length
- Particle shape, i.e., diameter and length
- High throughput, i.e., large volumes

Table 2. Qualitative ranking of candidate methods for handling and separation of mass quantities of BNNTs by AR. Both continuous and batch processes organized by function; E = Extraction; D = Deagglomeration; P = Purification; F = Fractionation.

Sorting Methodology			Particle Characteristics			Particle Sorting Capability		
Function, Device or Technique		Working Fluid	Nano-scale	Non-conductor	Fibrous Morphology	Size or Mass	Shape or AR	High Throughput
E	Inertial	Gas	😐	☺	☺	☺	☹	☺
	Cyclone	Gas/Vapor	😐	☺	☺	☺	☹	☺
D	High Shear	Liquid	☺	☺	☺	☹	☹	☺
	Fluidized Bed	Gas/Liquid	☺	☺	☺	☹	☹	☺
	Sonication	Liquid	☺	☺	☺	☹	☹	☺
	Ultrasonic Nozzle	Gas/Liquid	☺	☺	☺	☹	☹	☺
	Supercritical Fluids	Gas/Liquid	☺	☺	☺	☹	☹	☺
P	Tribo-Cyclone	Gas	😐	☺	☺	☺	☹	☺
	Electro-Cyclone	Gas/Vapor	😐	😐	☺	☺	☹	☺
	Hydro-Cyclone	Liquid	😐	☺	☺	☺	☹	☺
F	Electrophoresis	Liquid	☺	☺	☺	☺	☺	☹
	Acoustophoresis	Gas/Liquid	☺	☺	☺	☺	☺	☹
	Electrostatic	Gas/Vapor	😐	☺	☺	☺	☺	☺

Legend: ☺ = Yes; ☹ = No; 😐 = Perhaps

The extraction methods (E), inertial separators and gas cyclones, can isolate nanoscale particulate in clusters only and possess limited ability to sort by size or mass. Operation of inertial separators tends to be restricted to dry conditions, but cyclone separators are capable of operating in moist environments, i.e., particles suspended in vapor. The capability of more refined sorting by particle size can be enhanced by multiple units of varying geometry arranged in series.

The deagglomeration methods (D) have the same rankings and all operate under predominantly wet conditions. Some fluidized bed, ultrasonic nozzle, and SCF processing involves the transition of particle suspensions from the liquid to gas phase. All methods listed are capable of handling nanoscale particulate, but none are compatible with particle sorting by either size or morphology. Ultimately, the choice may come down to which method demonstrates the best results in terms of operability, reproducibility, and maintainability.

The purification methods (P) listed have similar rankings and separation efficiency decreases with particle size, particularly in the nanoscale range. In contrast with tribo- and hydro-cyclones, the performance of electro-cyclones is limited with non-conductive particulate. All of the methods are capable of isolating fibrous particulate by size or mass, but none are compatible with sorting by particle morphology.

The fractionation methods (F) are the only techniques listed capable of sorting non-conductive, fibrous particulate by morphology. Electrostatic separation may be the only technique capable of handling large volumes, but the efficiency of incumbent methods decreases with particle size. Electrostatic *classification* of analytical quantities of nanoparticulate by morphology is a proven technology. Development of complementary electrostatic *separation* technology has been restricted by the lack of demand for sorting of nanoscale particulate in mass quantities.

3. Leading Candidate for Fractionation

Electrostatic separation methodologies clearly emerge from this survey as the most promising approach to the fractionation of BNNTs by AR. Consequently, techniques that are capable of sorting nanoparticles by morphology, particularly in mass quantities, are the leading candidates.

3.1. Electrostatic Shape Separation

Although electrostatic separation methods are compatible with sorting of mass quantities of semi-conducting, irregular-shaped particulate by morphology, application to nanoparticle fractionation remains uncertain. However, a recent patent teaches purification, sorting, and alignment of nanofibers using electrostatic forces [ref. 120]. Consequently, the issue of whether electrostatic *separation* technology is sufficiently advanced for sorting of BNNTs by AR is addressed in figure 18. Electrostatic *classification* technology is closely related and applies the same physical principles to nanoparticle sorting. The aerosol manufacturing industry routinely employs differential mobility analyzers (DMAs) for establishing size distributions in plumes (figure 18(a)) [ref. 121]. Customarily employed to extract a specified, mono-disperse fraction from poly-disperse feedstock, DMAs are only capable of handling analytical quantities.

An emerging technology, less common in industry, employs modified DMAs to determine nanoparticle shape distributions. Figure 18(b) shows a configuration that permits partitioning by either length or diameter [ref. 122]. The multi-step process utilizes DMAs in tandem and allows differential collection of particles by AR. Figure 18(c) shows a more recent incarnation that permits partitioning by particle length and diameter simultaneously [ref. 123]. The single-step process exploits a pulsed-field DMA that allows particles to be extracted directly based on AR. The significance of the latter technique is that a spectrum of charges can be generated that depends on nanoparticle morphology alone. This innovation means that an opportunity exists to fractionate mass quantities of BNNTs by AR in dedicated operation. Indeed, another patent teaches the manipulation and subsequent isolation of high-AR molecular structures, such as nanotubes, based on differential electrostatic charge [ref. 124].

Electrostatic separation technology is widely used to sort semi-conductive materials in the minerals industry. Dry separators of the high-tension, rotating drum-type are preferable for processing mass quantities. The anatomy of a pilot plant facility is presented in figure 19 in order to illustrate the operating principles [ref. 125]. Raw product is fed onto a rotating drum which is the carrier, or grounded electrode. High tension is applied to positive, charging electrodes suspended above the drum. Figure 19(a) shows that particles pass through the charging zone, acquire differential charge, and adhere to the drum. During customary operations, particles are then selectively released from the rotating drum by various means:

- Centrifugal forces at the front of the drum
- Gravitational forces at the bottom of the drum
- A mechanical wiper at the rear of the drum
- A series of neutralizing/discharging electrodes around the drum (optional)

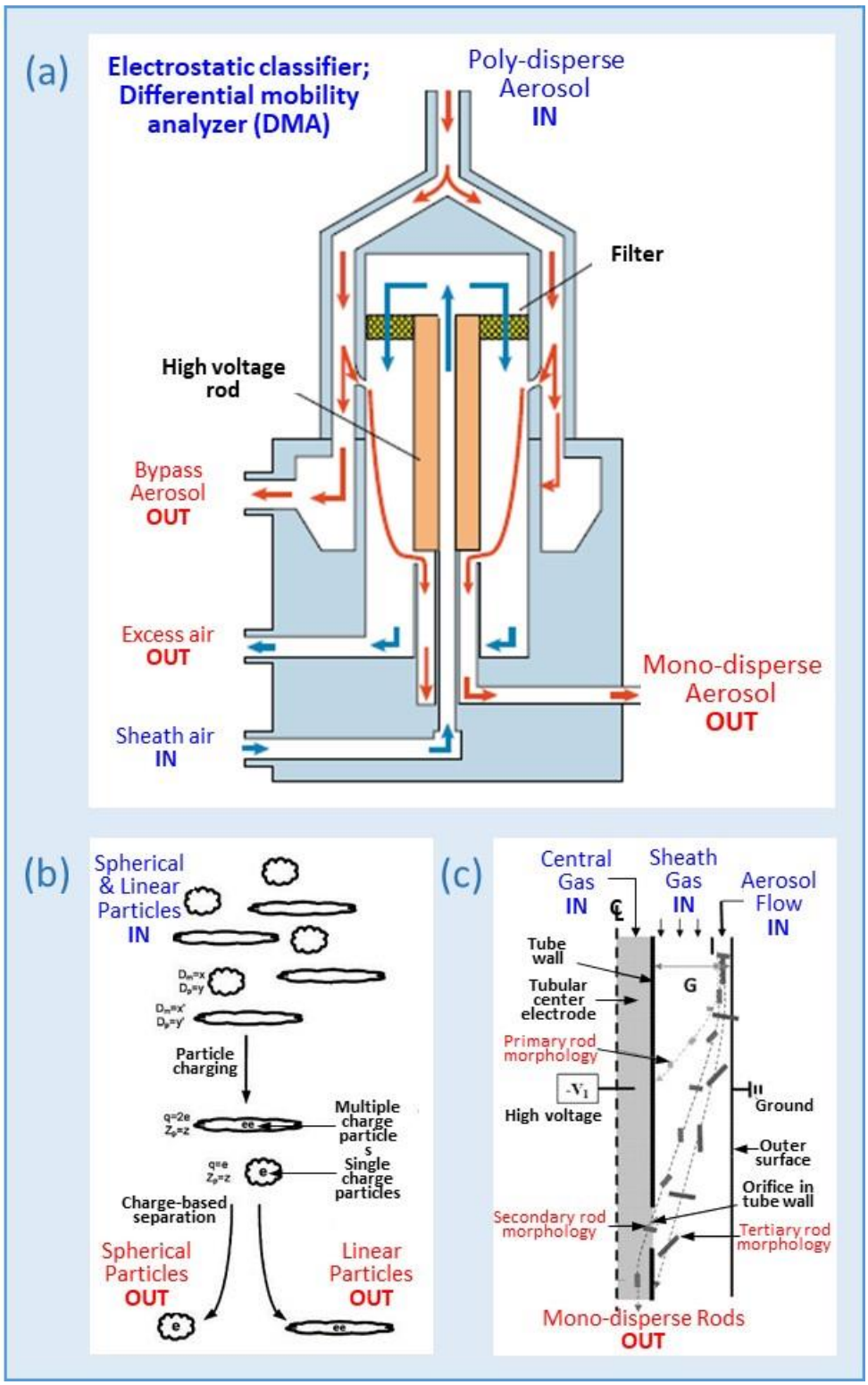

Figure 18. Electrostatic shape classification of nanoparticles; (a) differential mobility analysis (size-based) [ref. 121]; (b) sorting by length or diameter [ref. 122]; (c) sorting by length and diameter [ref. 123].

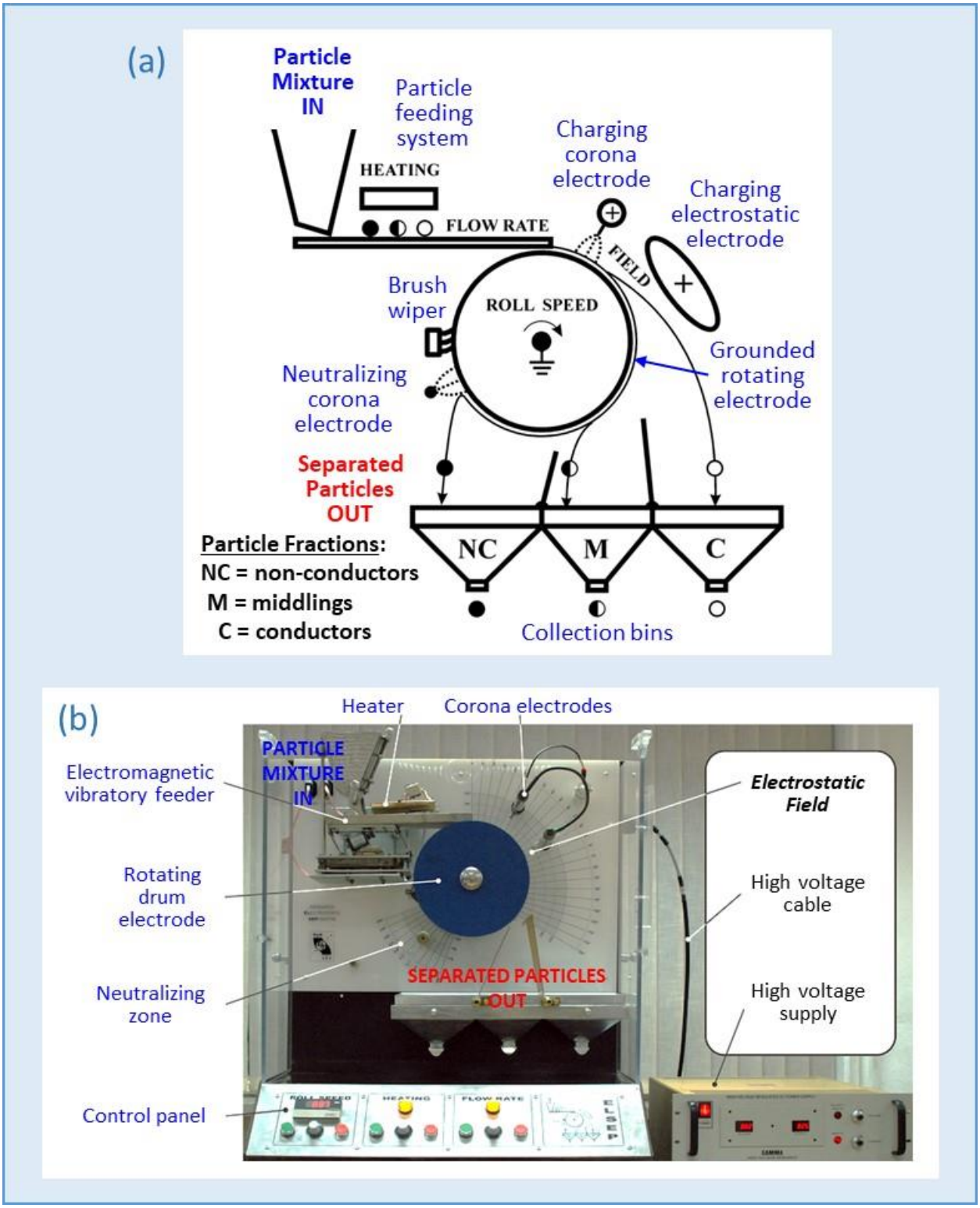

Figure 19. Electrostatic separation of particulate materials with *dissimilar* properties: High-tension, rotating drum separator for partitioning of mass quantities into 3 basic fractions; (a) process schematic; (b) equipment configuration [ref. 125].

Figure 19(b) indicates the equipment configuration governed by particle characteristics, such as mass, density, size or morphology [ref. 126]. The choice of electrodes depends on the electrical properties of the particles being separated. Particles are sorted based on differential surface conductivity and combinations of electrodes are customarily used to assure complete and uniform charging. Corona electrodes charge/discharge all of the particles, electrostatic electrodes charge/discharge conducting particles only. The majority of such separators are configured to separate dissimilar materials and create 3 basic fractions, namely conductors, non-conductors and middlings (a mixture). However, electrostatic shape separation of similar materials is also practical when the equipment configuration includes interchangeable rolls [ref. 127].

3.2. Relevant Case Study

The highlights of a case study by the Dascalescu group on electrostatic shape separation of flake mica ($\boldsymbol{M_f}$) from granular quartz ($\boldsymbol{Q_g}$) particles are presented in figure 20 [ref. 128]. Two configurations of a roll-type electrostatic separator are employed to partition the minerals based on particle morphology alone. Both types of particle are non-conductors, and separation relies on the acquisition of differential net charge. This is governed by both the surface area exposed to the charging corona electrode and the particle thickness. The principles that define the distinctly different approaches are as follows:

- Method #1 (figure 20(a)); employs a traditional, conductive roll and twin corona electrodes with opposite polarity. The first, positive electrode charges both the $\boldsymbol{M_f}$ and $\boldsymbol{Q_g}$ particles. All of the particles are attached to the negatively charged drum. The flat $\boldsymbol{M_f}$ particles acquire more net charge than the more spherical $\boldsymbol{Q_g}$ particles. The second, negative electrode is energized to selectively neutralize or discharge the $\boldsymbol{Q_g}$ particles, which are ejected *at the front* of the drum via centrifugal forces. The $\boldsymbol{M_f}$ particles remain adhered to the drum and the majority are removed *at the rear* by mechanical means.
- Method #2 (figure 20(b)); employs a less-common, non-conductive roll and a single corona electrode. Drum construction comprises a non-conducting surface with a conducting liner. Again, all of the $\boldsymbol{M_f}$ and $\boldsymbol{Q_g}$ particles are positively charged and adhere to the negatively charged drum. The lower net charge $\boldsymbol{Q_g}$ particles are ejected *toward the front* of the drum via centrifugal forces. The higher net charge $\boldsymbol{M_f}$ particles remain on the drum and the majority are released *toward the rear* via gravitational forces.

The implications of these operating principles for sorting of BNNTs by morphology are addressed in figure 21 [ref. 129]. The differential in electrostatic forces acting on high-AR flakes (f) vs. low AR granules (g) derives from:

- Higher exposed surface area;
  - higher net charge (**q**) => $\mathbf{q_f > q_g}$
- Reduced material thickness;
  - shorter isolating distance (**d**) => $\mathbf{d_f < d_g}$

In adapting roll-type electrostatic separation to BNNTs, length will govern the net charge, diameter will govern the isolating distance, and length/distance will determine the net pinning force. Consequently, the creation of a differential pinning force introduces the opportunity to fractionate BNNTs based on AR.

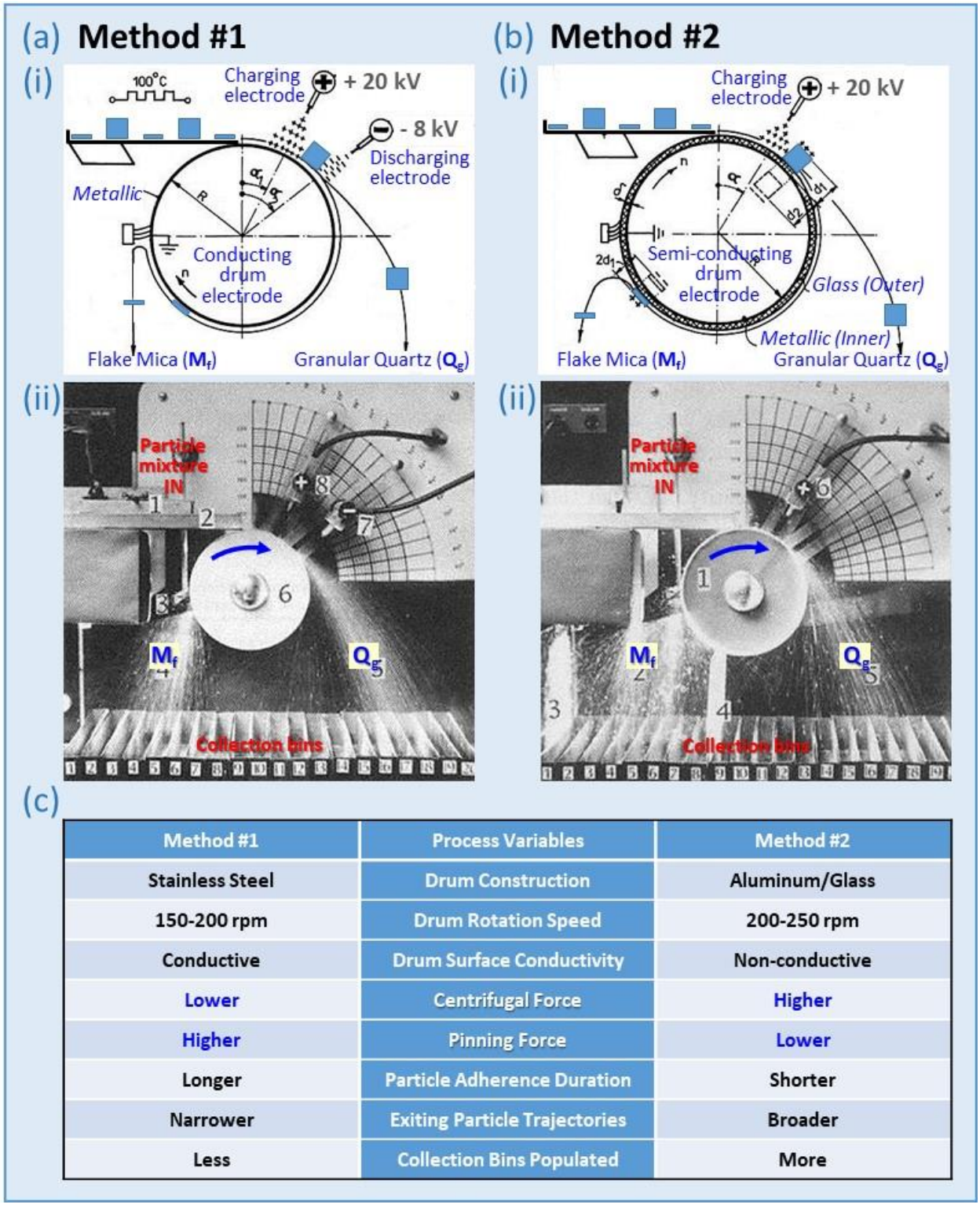

Method #1	Process Variables	Method #2
Stainless Steel	Drum Construction	Aluminum/Glass
150-200 rpm	Drum Rotation Speed	200-250 rpm
Conductive	Drum Surface Conductivity	Non-conductive
Lower	Centrifugal Force	Higher
Higher	Pinning Force	Lower
Longer	Particle Adherence Duration	Shorter
Narrower	Exiting Particle Trajectories	Broader
Less	Collection Bins Populated	More

Figure 20. Electrostatic shape separation of materials with *similar* properties; flake mica (M_f) from granular quartz (Q_g) [ref. 128]. Partitioning of multiple fractions into an array of collection bins; (a) uncoated, conducting drum, (b) coated, semi-conducting drum; (c) comparison of performance.

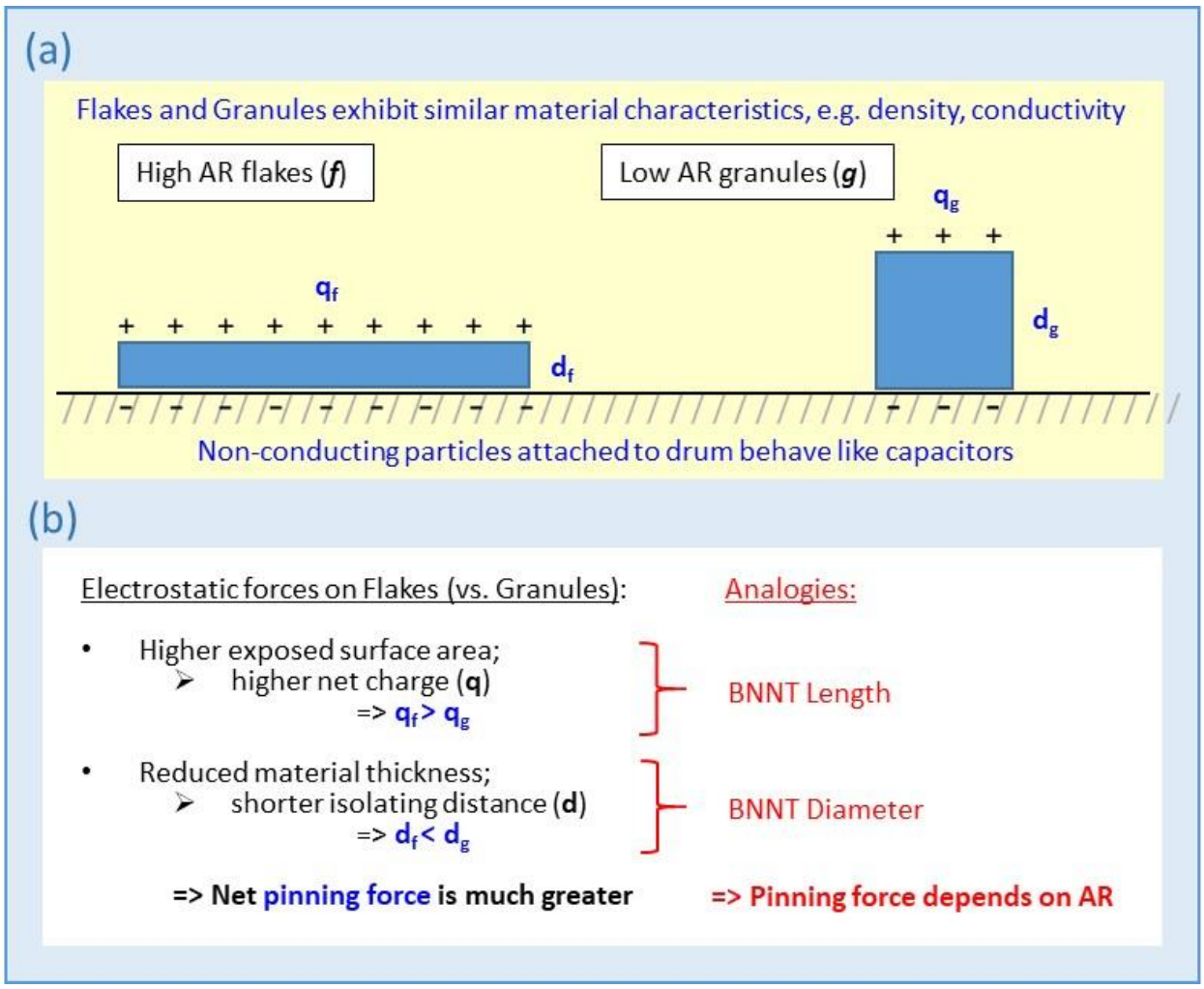

Figure 21. Electrostatic shape separation; (a) dependence of pinning force on particle morphology; (b) implications for fractionation of BNNTs by AR.

The charging electrode excitation and the drum construction control the initial strength and rate of decay of the pinning force. The drum rotation speed controls the centrifugal force which is constant. The range of exiting particle trajectories will depend on the increasing difference between these attractive and repulsive forces. Theoretically, establishing the appropriate differential will maximize the yield of BNNTs with lengths surrounding the targeted AR. Although partitioning into relatively coarse fractions might be the reality, a tighter length distribution may be achieved by incorporating a series of neutralizing corona electrodes. In addition, the use of multiple devices in-tandem may permit separation into even finer fractions following a single, partitioning operation.

3.3. Commercial Equipment

In the final analysis, electrostatic shape separation technology offers the highest potential for sorting of BNNTs by AR. Corona charging, rotating drum separators are traditionally employed to partition large volumes of mm-sized particles comprising dissimilar materials into limited shape fractions. A selection of commercial rotating drum-type electrostatic separators that may be modified to perform such a function is presented in figure 22 [refs. 130, 131, and 132].

Operating details of the currently available equipment that is designed for pilot plant or research applications are listed below:

- ***OUTOTEC; Carpco EHTP 111-15 [ref. 130]***
    - Interchangeable 25 cm and 35 cm diameter steel rolls (15 cm wide) with infrared heating capability
    - Two DC pinning electrodes (40 kV), one AC discharging electrode (18 kV), and a tension grounded roll brush for particle removal
    - Particle sizes; 75 µm to 10 mm
    - Capacity; 150 kg/hr
    - Cost; ~ $75,000

- ***ERIEZ; HTES 533 [ref. 131]***
    - 35 cm diameter stainless steel roll (15 cm wide)
    - One DC electrode (40 kV), cleaning brush, but no AC cleaning electrode for particle removal
    - Particle sizes; 100 µm to 10 mm
    - Capacity; 50 kg/hr
    - Cost; ~ $65,000

- ***OREKINETICS; Corona Stat 100 [ref. 132]***
    - 25 cm diameter steel roll (15 cm wide), feed temp = 80–150°C
    - One DC electrode (15–25 kV), one AC wiping electrode, and a cleaning brush for particle removal
    - Particle sizes; 50 µm to 400 µm
    - Capacity; 150 kg/hr
    - Cost; ~ $20,000

Figure 22. Corona charging/rotating drum electrostatic separators - commercial, pilot plant equipment; (a) Carpco EHTP 111-15 [ref. 130]; (b) Eriez HTES 533 [ref. 131];(c) OreKinetics Corona Stat 100 [ref. 132].

4. Concluding Remarks

This technology survey elevates the topic of fractionating high-AR BNNTs in large volumes for use in discontinuously reinforced MMCs. The qualitative evaluation of particle-sorting methodologies is intended to trigger discussion on shape-based fractionation of quantities compatible with commercial applications. Incumbent techniques can be applied to fibrous, nanoscale particles, but tend to be incompatible with handling mass quantities. Although high-tension separators have proven effective with sub-micron particles, equipment has yet to be configured for sorting nanoparticulate, particularly nanotubes.

The case for electrostatic fractionation of BNNTs by AR using a high-tension, corona-charging, rotating drum separator is presented. The opportunity for innovation derives from the fact that equipment for shape separation of a single, non-conductive material in nanofiber form is not commercially available. As a consequence, fractionation of BNNTs will require adaptation of current electrostatic separation/classification techniques to partition mass quantities of nm-sized particles with a fibrous morphology.

Separation efficacy may be enhanced by formulating a sequence of neutralizing, corona electrodes capable of creating multiple close fractions in a single sorting operation (replacing multiple separators). Further, using semi-conductive roll construction offers the additional capability of operating under either dry or moist conditions. Concentrating developmental efforts on a single methodology that is compatible with in-flight and post-synthesis operations would be prudent. Integration of the various functions (extracting, deagglomerating, purifying, and fractionating) to create either a dry, continuous process or a wet, batch process is recommended.

It is evident that the availability of copious quantities of BNNTs has heightened interest in structural composite applications. However, the future of BNNT-MMCs has many skeptics, and there is an enduring sentiment that using nanotubes to create "superstrong" materials is science fiction [ref. 133]. Key to the success of BNNT-MMCs as load-bearing materials will be the ability to exploit the properties of individual nanotubes (on the microscale) in arrays embedded in matrices (on the macroscale). Consequently, a ready source of high-AR, low-defect BNNTs represents an important first step toward achieving that objective. Even if not the primary reinforcing agent, such BNNTs may still be utilized to supplement the mechanical or physical properties of fiber-reinforced composites [ref. 134].

Endnote:

This report represents the final installment of a trilogy addressing induction plasma synthesis and post-synthesis processing of mass quantities of BNNTs. The previous installments comprise;

> S.J. Hales, J.A. Alexa, B.J. Jensen, and D.L. Thomsen, ***Radio Frequency Plasma Synthesis of Boron Nitride Nanotubes (BNNTs) for Structural Applications: Part I***, NASA/TP–2016-219001, Langley Research Center, Hampton, VA, 33 pp., January 2016.
>
> S.J. Hales, J.A. Alexa, and B.J. Jensen, ***Radio Frequency Plasma Synthesis of Boron Nitride Nanotubes (BNNTs) for Structural Applications: Part II***, NASA/TP–2016-219194, Langley Research Center, Hampton, VA, 40 pp., May 2016.

5. References

1. A.R. Harutyunyan, "Synthesis of small diameter single-walled carbon nanotubes," Honda Motor Co. Ltd., Japan, US Patent # 7,981,396, July 19, 2011.
2. S.E. Iyuke, "Process for producing carbon nanotubes," South Africa, US Patent # 9,102,525, August 11, 2015.
3. R.D. Denton, D.B. Noyes, R.J. Koveal, and T.A. Ring, "Removing carbon nanotubes from a continuous reactor effluent," ExxonMobil, Houston, TX, US Patent # 10,343,104, July 9, 2019.
4. E. Joselevich, H. Dai, J. Liu, K. Hata, and A.H. Windle, "Carbon nanotube synthesis and organization," in ***Carbon Nanotubes: Advanced topics in the synthesis, structure, properties and applications***, A. Jorio, G. Dresselhaus, and M.S. Dresselhaus (eds.), Springer-Verlag, Germany, pp. 101-165, 2008.
5. M.J. Schulz, V. Shanov, Z. Yin, and M. Cahay (eds.), ***Nanotube Superfiber Materials***, Elsevier, Cambridge, MA, 2nd Edition, 972 pp., 2019.
6. M.B. Jakubinek ..... and B. Simard, "Polymer nanocomposites incorporating boron nitride nanotubes, "TechConnect Briefs, Adv. Mater., vol. 1, pp. 416-419, 2015.
7. "Commercializing boron nitride nanotubes (BNNTs) for the advanced engineering materials industry," (J. Pollak with A. Chilton), https://www.azonano.com/article.aspx?ArticleID=4144 Accessed September 3 2020.
8. C.E. Harris, M.J. Shuart, and H.R. Gray, "A survey of emerging materials for revolutionary aerospace vehicle structures and propulsion systems", NASA/TM-2002-211664, Langley Research Center, Hampton, VA, May 2002.
9. J.N. Coleman, U. Khan, W.J. Blau, and Y.K. Gun'ko, "Small but strong: A review of the mechanical properties of carbon nanotube–polymer composites," Carbon, vol. 44, no. 9, pp. 1624-1652, 2006.
10. M. Pell, J.B. Dunson, and E.M. Knowlton, "Gas-solid operations and equipment," in ***Perry's Chemical Engineers' Handbook***, D.W. Green and R.H. Perry (eds.), McGraw-Hill, New York, NY, 8th Edition, Section 17, 59 pp., 2008.
11. R. Dolbec, "Boron nitride nanotubes: properties, synthesis and applications," Sigma-Aldrich, Inc., https://www.sigmaaldrich.com/technical-documents/articles/technology-spotlights/boron-nitride-nanotubes.html Accessed September 3, 2020.
12. M.B. Jakubinek ..... and B. Simard, "Assessment of boron nitride nanotube materials using X-ray photoelectron spectroscopy," Canadian J. Chemistry, vol. 97, no. 6, pp. 457-464, 2019.
13. J.E. Lundquist and A. Thomas, "Inertial separator," Pall Corp, Port Washington, NY, US Patent # 7,879,123, February 1, 2011.
14. "Cyclonic separation," *Wikipedia, The Free Encyclopedia*, last modified August 29, 2020, https://en.wikipedia.org/wiki/Cyclonic_separation Accessed September 3, 2020.
15. A.B. Cecala ….. and M.J. Schultz, "Air cleaning devices," ***Dust Control Handbook for Industrial Minerals Mining and Processing***, NIOSH, Pittsburgh, PA, Report of Investigations 9689, pp. 28-43, January 2012.
16. A. Alves, J. Paiva, and R.L.R. Salcedo, "Cyclone optimization including particle clustering," Powder Technol., vol. 272, no. 3, pp. 14-22, 2015.
17. J. Zhang, S. Xu, and W. Li, "High shear mixers: A review of typical applications and studies on power draw, flow pattern, energy dissipation and transfer properties," Chem. Eng. & Proc.: Process Intensification, vols. 57-58, no. 33, pp. 25-41, 2012.

18. J. Baldyga ….. and G. Padron, "Dispersion of nanoparticle clusters in a rotor-stator mixer," Ind. & Eng. Chem. Res., vol. 47, no. 10, pp. 3652-3663, 2008a.
19. C. Banaszek, "Mixing nanomaterials," Ceramic Industry, vol. 160, no. 11, pp. 9-12, 2010.
20. "High-shear mixer," *Wikipedia, The Free Encyclopedia*, last modified June 3, 2020, https://en.wikipedia.org/wiki/High-shear_mixer Accessed September 3, 2020.
21. "High speed powder induction-Inline," Charles Ross & Son Co., Hauppauge, NY, https://www.mixers.com/ Accessed September 3, 2020.
22. "High shear in-line mixers," Silverson Machines, Inc., East Longmeadow, MA, https://www.silverson.com/ Accessed September 3, 2020.
23. A. Graf ….. and J. Zaumseil, "Large scale, selective dispersion of long single-walled carbon nanotubes with high photoluminescence quantum yield by shear force mixing," Carbon, vol. 105, no. 8, pp. 593-599, 2016.
24. "Fluidization," *Wikipedia, The Free Encyclopedia*, last modified July 10, 2020, https://en.wikipedia.org/wiki/Fluidization Accessed September 3, 2020. [Public domain]
25. R.P. Chhabra and M.G. Basavaraj (eds.), "Fluidisation", ***Coulson and Richardson's Chemical Engineering,*** Butterworth-Heinemann, Oxford, UK, 6th Edition., Vol. 2A, Ch. 9, pp. 449-554, 2019.
26. S.W. Kim, "Effect of particle size on carbon nanotube aggregates behavior in dilute phase of a fluidized bed," J. Processes, vol. 6, no. 8, Article ID 121, 12 pp., 2018.
27. J.R. van Ommen, J.M. Valverde, and R. Pfeffer, "Fluidization of nanopowders: A review," J. Nanopart. Res., vol. 14, no. 3, pp. 737-766, 2012.
28. K.G. Dassios ….. and T.E. Matikas, " Optimization of sonication parameters for homogeneous surfactant-assisted dispersion of multiwalled carbon nanotubes in aqueous solutions," Phys. Chem. C, vol. 119, no. 13, pp. 7506-7516, 2015.
29. R. Dave ….. and M.S. Tomassone, "Deagglomeration and mixing of nanoparticles," Proc. NSF Nanoscale Sci. & Eng. Conf., Washington, DC, 3 pp., December 2006.
30. R. Pfeffer ..... and C. Zhu, "System and method for nanoparticle and nanoagglomerate fluidization," New Jersey Inst. of Technol., NJ, US Patent # 7,658,340, February 9, 2010.
31. T. Hielscher, Ha. Hielscher, and Ho. Hielscher, "Apparatus and method for treating fluids with ultrasound," Hielscher GmbH, Germany, US Patent Application # 2015/0071023 A1, March 12, 2015.
32. "Sonication," *Wikipedia, The Free Encyclopedia*, last modified July 22, 2020, https://en.wikipedia.org/wiki/Sonication Accessed September 3, 2020. [Created by Peshkovs; "Schematic of bench and industrial-scale ultrasonic liquid processors produced by Industrial Sonomechanics, LLC," image subject to https://creativecommons.org/licenses/by-sa/3.0/].
33. "Ultrasonic dispersing and deagglomeration," Hielscher Ultrasonics GmbH, 14513 Teltow, Germany, https://www.hielscher.com/ Accessed September 3, 2020.
34. A. Sesis ..... and G. Hinds, "Influence of acoustic cavitation on the controlled ultrasonic dispersion of carbon nanotubes," J. Phys. Chem. B, vol. 117, Article ID 15141, 16 pp., 2013.
35. "Ultrasonic nozzle systems," Sono-Tek Corp., Milton, NY, https://www.sono-tek.com/ Accessed September 3, 2020.
36. "Ultrasonic nozzle," *Wikipedia, The Free Encyclopedia*, last modified July 20, 2020, https://en.wikipedia.org/wiki/Ultrasonic_nozzle Accessed September 3, 2020.
37. "Supercritical fluid," *Wikipedia, The Free Encyclopedia*, last modified September 1, 2020, https://en.wikipedia.org/wiki/Supercritical_fluid Accessed September 3, 2020.

38. M. Vazquez da Silva, “Supercritical fluids and its applications,” in ***Current Trends in Chemical Engineering***, J.M.P.Q. Delgado (ed.), Studium Press LLC, Houston, TX, Ch. 10, pp. 293-312, 2010.
39. R. Parhi and P. Suresh, “Supercritical fluid technology: A review,”, Adv. Pharm. Sci. & Technol., vol. 1, no. 1, pp. 13-36, 2013. [Open Access Pub, licensed under https://creativecommons.org/licenses/by/4.0/ ; Image unchanged].
40. Y.P. Sun, “Aqueous suspension of nanoscale drug particles from supercritical fluid processing,” Clemson University, SC, US Patent # 7,754,243, July 13, 2010.
41. D. To, “Nanoparticle mixing through rapid expansion of high pressure and supercritical suspensions,” J. Nanopart. Res., vol. 13, no. 9, pp. 4253-4266, 2011.
42. G.P. Sanganwar ….. and R.N. Dave, "Environmentally benign nanomixing by sonication in high pressure carbon dioxide," J. Nanopart. Res., vol. 11, no. 2, pp. 405-419, 2009.
43. W.R. Jung ….. and Y.S. Seo, "Reduced damage to carbon nanotubes during ultrasound-assisted dispersion as a result of supercritical-fluid treatment," Carbon, vol.50, no. 2, pp. 633-636, 2012.
44. J.P. Quigley, K. Herrington, M. Bortner, and D.G. Baird, "Benign reduction of carbon nanotube agglomerates using a supercritical carbon dioxide process," Appl. Phys. A, vol. 117, no. 3, pp. 1003-1017, 2014.
45. M. Turk, “Manufacture of submicron drug particles with enhanced dissolution behavior by rapid expansion processes,” Supercritical Fluids, vol. 47, no. 3, pp. 537-545, 2009.
46. T.J. Young, S. Mawson, and K.P. Johnston, "Rapid expansion from supercritical to aqueous solution to produce submicron suspensions of water-insoluble drugs," Biotechnol. Prog., vol. 16, no. 3, pp. 402-407, 2000.
47. Z. Liu and B. Han, “Synthesis of carbon-nanotube composites using supercritical fluids and their potential applications,” Adv. Mater., vol. 21, no. 7, pp. 825-829, 2009.
48. S. Matsusaka, H. Maruyama, T. Maruyama, and M. Ghadiri, “Triboelectric charging of powders: A review,” Chemical Engineering Science, vol. 65, no. 22, pp. 5781-5807, 2010.
49. G. Dodbiba, A. Shibayama, T. Miyasaki, and T. Fujita, “Triboelectrostatic separation of ABS, PS and PP plastic mixture,” Mater. Trans., JIM, vol. 44, no. 1, pp. 161-166, 2003.
50. M.E. Zelmat ..... and L. Dascalescu, “Experimental comparative study of different tribocharging devices for triboelectric separation of insulating particles,” IEEE Trans. Indust. Appl., vol. 49, no. 3, pp. 1113-1118, 2013.
51. D.J. Lacks and A. Levandovsky, “Effect of particle size distribution on the polarity of triboelectric charging in granular insulator systems,” Electrostatics, vol. 65, no. 2, pp. 107-112, 2007.
52. P.M. Ireland, " Dynamic particle-surface tribocharging: The role of shape and contact mode," Electrostatics, vol. 70, no. 6, pp. 524-531, 2012.
53. F. Daniel, M. Pourprix, J. Vendel, J.Y. Deysson, and J.N. Dumont, “The electrocyclone – a new pre-filtration technique,” ***Gaseous Effluent Treatment in Nuclear Installations***, G. Fraser and F. Luykx (eds.), Graham & Trotman, London, UK, pp. 601-613, 1986.
54. W. Peukert and C. Wadenpohl, "Industrial separation of fine particles with difficult dust properties," Powder Technol., vol. 118, nos. 1-2, pp. 136-148, 2001.
55. A. Jaworek, A. Krupa, and T. Czech, “Modern electrostatic devices and methods for exhaust gas cleaning: A brief review,” Electrostatics, vol. 65, no. 3, pp. 133-155, 2007.

56. K.S. Lim, H.S. Lim, and K.W. Lee, "Comparative performances of conventional cyclones and a double cyclone with and without an electric field," Aerosol Sci., vol. 35, no. 1, pp. 103-116, 2004.
57. G.Y. Lin ..... and F.T. Chang, "High-efficiency wet electrocyclone for removing fine and nanosized particles," Separation & Purification Technol., vol.114, no. 8, pp. 99-107, 2013.
58. "Hydrocyclone," *Wikipedia, The Free Encyclopedia*, last modified January 19, 2020, https://en.wikipedia.org/wiki/Hydrocyclone Accessed September 3, 2020.
59. "Hydrocyclones," *Thermopedia, The Most Reliable Source for Thermodynamics, Heat Transfer, Fluid Flow Science and Technologies*, last modified February 14, 2011, http://thermopedia.com/content/862/ Accessed September 3, 2020.
60. Q. Yang, H. Wang, and Z. Li, "Solid/liquid separation performance of hydrocyclones with different cone combinations," Separation & Purification Technol., vol. 74, no. 3, pp. 271-279, 2010.
61. G.A. Young, "Tangentially staged hydrocyclones," Amoco Corp., Chicago, IL, US Patent # 4,711,720, December 8, 1987.
62. S. Khare and M. Dell'Amico, "An overview of solid-liquid separation of residues from coal liquefaction processes," Canadian J. Chem. Eng., vol. 91, no. 2, pp. 324-331, 2013.
63. M.F. Dlamini, M. S. Powell, and C. J. Meyer. "A CFD simulation of a single phase hydrocyclone flow field," J. South African Inst. Min. & Metall., vol. 105, no. 10, pp. 711-717, 2005.
64. R.D. Denton, D.B. Noyes, R.J. Koveal, and T.A. Ring, "Removing carbon nanotubes from a water system," ExxonMobil, Houston, TX, US Patent # 9,975,793, May 22, 2018.
65. "Electrophoresis," *Wikipedia, The Free Encyclopedia*, last modified August 8, 2020, https://en.wikipedia.org/wiki/Electrophoresis Accessed September 3, 2020.
66. Field flow fractionation," *Wikipedia, The Free Encyclopedia*, last modified April 14, 2020, https://en.wikipedia.org/wiki/Field_flow_fractionation Accessed September 3, 2020. [Created by Analysis fellow; "Flow field-flow fractionation (AF4) channel cross section," image subject to https://creativecommons.org/licenses/by-sa/3.0/].
67. T. Salafi, K.K. Zeming, and Y. Zhang, "Advancements in microfluidics for nanoparticle separation," Lab on a Chip (RSC), vol. 17, no. 1, pp. 11-33, 2017.
68. D.R. Gossett ..... and D. Di Carlo, "Label-free cell separation and sorting in microfluidic systems," Anal. Bioanal. Chem., vol. 397, no. 8, pp. 3249-3267, 2010.
69. D.A. Heller ..... and M.S. Strano, "Concomitant length and diameter separation of single-walled carbon nanotubes," J. Am. Chem. Soc., vol. 126, no. 44, pp. 14567-14573, 2004.
70. M.C. Hersam, "Progress towards monodisperse single-walled carbon nanotubes," Nat. Nanotechnol., vol. 3, no. 7, pp. 387–394, 2008.
71. "Field flow fractionation," *Wikipedia, The Free Encyclopedia*, last modified April 14, 2020, https://en.wikipedia.org/wiki/Field_flow_fractionation Accessed September 3, 2020.
72. J. Chun, J.A. Fagan, E.K. Hobbie, and B.J. Bauer, "Size separation of single-wall carbon nanotubes by flow-field flow fractionation," Anal. Chem., vol. 80, no. 7, pp. 2514-2523, 2008.
73. B. Chen and J.P. Selegue, "Separation and characterization of single-walled and multi-walled carbon nanotubes by using flow field-flow fractionation," Anal. Chem., vol. 74, no. 18, pp. 4774-4780, 2002.

74. M. Alfi and J. Park, “Theoretical analysis of the local orientation effect and the lift-hyperlayer mode of rodlike particles in field-flow fractionation,” J. Separation Sci., vol. 37, no. 7, pp. 876-883, 2014.
75. S.H. Kim and M.R. Zachariah, “In-flight size classification of carbon nanotubes by gas phase electrophoresis,” Nanotechnology, vol. 16, no. 10, pp. 2149-2152, 2005.
76. F. Petersson, L. Aberg, A.M. Sward-Nilsson, and T.J. Laurell, “Free flow acoustophoresis: Microfluidic-based mode of particle and cell separation,” Anal. Chem., vol. 79, no. 14, pp. 5117-5123, 2007.
77. R.S. Budwig, M.J. Anderson, G. Putnam, and C. Manning, "Ultrasonic particle size fractionation in a moving air stream," Ultrasonics, vol. 50, no. 1, pp. 26-31, 2010.
78. R.J. Imani and E. Robert, “Acoustic separation of submicron solid particles in air,” Ultrasonics, vol. 63, no. 12, pp. 135-140, 2015.
79. A. Lenshof, C. Magnusson, and T. Laurell, “Acoustofluidics 8: Applications of acoustophoresis in continuous flow microsystems,” Lab on a Chip (RSC), vol. 12, no. 7, pp. 1210-1223, 2012.
80. T.J. Laurell, F. Petersson, and A.M. Sward-Nilsson, "Chip integrated strategies for acoustic separation and manipulation of cells and particles," Chem. Soc. Rev., vol. 36, no. 3, pp. 492-506, 2007.
81. J.S. Heyman, "Acoustophoresis separation method," NASA, DC, US Patent # 5,192,450, March 9, 1993.
82. M. Wu ..... and T.J. Huang, “Acoustic separation of nanoparticles in continuous flow,” Adv. Funct. Mater., vol. 27, no. 14, Article ID 1606039, 18 pp., 2017.
83. J. Dionne, B. Lipkins, and E.A. Rietman, “High-volume fast separation of multi-phase components in fluid suspensions,” FloDesign Sonics, Inc, Wilbraham, MA, US Patent # 9,421,553, August 23, 2016.
84. K.R. Parker, “Why an electrostatic precipitator ?,” ***Applied Electrostatic Precipitation***, K.R. Parker (ed.), Chapman & Hall, New York, NY, 1st Edition, Ch. 1, pp. 1-10, 1997.
85. “Electrostatic precipitator,” *Wikipedia, The Free Encyclopedia*, last modified August 29, 2020, https://en.wikipedia.org/wiki/Electrostatic_precipitator, Accessed September 3, 2020.
86. “Electrostatic separator,” *Wikipedia, The Free Encyclopedia*, last modified June 26, 2020, https://en.wikipedia.org/wiki/Electrostatic_separator, Accessed September 3, 2020.
87. E.G. Kelly and D.J. Spottiswood, “The theory of electrostatic separations: A review – Part I. Fundamentals,” Minerals Engineering, vol. 2, no. 1, pp. 33-46, 1989a.
88. E.S. Yan, T.J. Grey, and K.R. McHenry, “High-tension electrostatic classifier and separator, and associated method,” Outokumpu, Finland, US Patent # 6,797,908, September 28, 2004.
89. F.S. Knoll and J.B. Taylor, “Advances in electrostatic separation,” Minerals & Metallurgical Processing, vol. 2, no. 2, pp. 106-113, 1985.
90. E.G. Kelly and D.J. Spottiswood, “The theory of electrostatic separations: A review – Part II. Particle charging,” Minerals Engineering, vol. 2, no. 2, pp. 193-205, 1989b.
91. E.G. Kelly and D.J. Spottiswood, “The theory of electrostatic separations: A review – Part III. The separation of particles,” Minerals Engineering, vol. 2, no. 3, pp. 337-349, 1989c.
92. X.Z. Ming, L. Jia, L.H. Zhou, and W. Jiang, “Dynamics of conductive and nonconductive particles under high-voltage electrostatic coupling fields,” Science in China E: Technological Sciences, vol. 52, no. 8, pp. 2359-2366, 2009.
93. A. Gupta and D. Yan (eds.), “Magnetic and electrostatic separation,” ***Mineral Processing Design and Operations***, Elsevier, Cambridge, MA, 2nd Edition, Ch. 17, pp. 629-687, 2016.

94. P.A. Baron, G.J. Deye, and J. Fernback, "Length separation of fibers," Aerosol Sci. & Tech., vol. 21, no. 2, pp. 179-192, 1994.
95. C.E. Jordan and C.P. Weaver, "System for the dielectrophoretic separation of particulate and granular material," Washington, DC, US Patent # 4,100,068, July 11, 1978.
96. C.E. Jordan and G.V. Sullivan, "Dielectric separation of minerals," US Bureau of Mines Bulletin, No. 685, 22 pp., 1985.
97. K.S. Lindley and N.A. Rowson, "Feed preparation factors affecting the efficiency of electrostatic separation," Magnetic & Electrical Separation, vol. 8, no. 3, pp. 161-173, 1997.
98. F.S. Knoll, "Method of separating vermiculite from the associated gangue," Jacksonville, FL, US Patent # 4,247,390, January 27, 1981.
99. H. Daiku, M. Tsukahara, T. Inoue, and H. Maehata, "Apparatus for separating plastic chips," Hitachi Zosen Corp., Japan, US Patent # 6,903,294, June 7, 2005.
100. C.J. Unrau, R.L. Axelbaum, P. Biswas, and P. Fraundorf, "Online size characterization of nanofibers and nanotubes," in ***Molecular Building Blocks for Nanotechnology***, Springer, New York, NY, Ch. 9, pp. 212-245, 2007.
101. S.R. Bakshi and A. Agarwal, "An analysis of the factors affecting strengthening in carbon nanotube reinforced aluminum composites", Carbon, vol. 49, pp. 533-544, 2011.
102. K.S. Munir, P. Kingshott, and C. Wen, "Carbon nanotube reinforced titanium metal matrix composites prepared by powder metallurgy - A review," Crit. Rev. Solid State & Mater. Sci., vol. 40, no. 1, pp. 38-55, 2015.
103. D. Lahiri ..... and A. Agarwal," Insight into reactions and interface between boron nitride nanotubes and aluminum", Mater. Res., vol. 27, no. 21, pp. 2760-2770, 2012.
104. M.M.H. Bhuiyan, L.H. Li, J. Wang, P. Hodgson, and Y. Chen, "Interfacial reactions between titanium and boron nitride nanotubes," Scripta Mater., vol. 127, pp. 108-112, 2017.
105. S.K. Singhal, A.K. Srivastava, R. Pasricha, and R.B. Mathur, "Fabrication of Al-matrix composites reinforced with amino functionalized boron nitride nanotubes," Nanosci. & Nanotechnol., vol. 11, no. 6, pp. 5179-5186, 2011.
106. S. Abbas ..... and C. Tang, "Synthesis of boron nitride nanotubes using an oxygen and carbon dual-free precursor," RSC Adv., vol. 8, no. 8, pp. 3989-3995, 2018.
107. J. Baptista, "4 steps to effective pigment dispersions," Coatings SA, vol. 6, no. 2, pp. 40-43, 2018.
108. J. Liu, L.-Q. Wang, W.D. Samuels, and G.J. Exarhos, "Aggregation and dispersion of colloidal suspensions by inorganic surfactants: Effect of chemical speciation and molecular conformation," Phys. Chem. B, vol. 101, no. 41, pp. 8264-8269, 1997.
109. A.L. Tiano ..... and C.C. Fay, "Boron nitride nanotube: synthesis and applications," ***Nanosensors, Biosensors, and Info-Tech Sensors and Systems***, V.K. Varadan (ed.), Proc. of SPIE, vol. 9060, Article ID 906006, 19 pp., 2014.
110. C.M. Hansen, ***Hansen Solubility Parameters: A User's Handbook***, CRC Press , Boca Raton, FL, Second Edition, 544 pp., 2007.
111. S.D. Bergin, Z. Sun, D. Rickard, P.V. Streich, J.P. Hamilton, and J.N. Coleman, "Multicomponent solubility parameters for single-walled carbon nanotube - solvent mixtures," ACS Nano, vol. 3, no. 8, pp. 2340-2350, 2009.
112. Y. Hernandez, M. Lotya, D. Rickard, S.D. Bergin, and J.N. Coleman, "Measurement of multicomponent solubility parameters for graphene facilitates solvent discovery," Langmuir, vol. 26, no. 5, pp. 3208-3213, 2009.

113. J.M.G. Cowie, M.A. Mohsin, and I.J. McEwen, "Alcohol-water cosolvent systems for poly(methyl methacrylate)," Polymer, vol. 28, no. 9, pp. 1569-1572, 1987.
114. C. S. Torres-Castillo, C. Bruel and J. R. Tavares, "Chemical affinity and dispersibility of boron nitride nanotubes," Nanoscale Adv., vol. 2, no. 6, pp. 2497-2506, 2020.
115. C.Y. Zhi, ... and D. Golberg, "Chemically activated boron nitride nanotubes," Chem. Asian J., vol. 4, no. 10, pp. 1536-1540, 2009.
116. J. Guan, K.S. Kim, M.B. Jakubinek, and B. Simard, "pH-switchable water-soluble boron nitride nanotubes," Chemistry Select, vol. 3, no. 32, pp. 9308-9312, 2018.
117. S. Ramesh ..... and R.E. Smalley, "Dissolution of pristine single-walled carbon nanotubes in superacids by direct protonation,". Phys. Chem. B, vol. 108, no. 26, pp. 8794−8798, 2004.
118. M.J. Green ..... and M. Pasquali, "Direct imaging of carbon nanotubes spontaneously filled with solvent," Chem. Comm., vol. 47, no. 4, pp. 1228−1230, 2011.
119. O. Kleinerman ..... and Y. Talmon, "Dissolution and characterization of boron nitride nanotubes in superacid," Langmuir, vol. 33, no. 50, pp. 14340-14346, 2017.
120. D.C. Eberlein and R.H. Detig, "System and method for the manipulation, classification sorting, purification, placement, and alignment of nano fibers using electrostatic forces and electrographic techniques," Electrolux Corp., New Providence, NJ, US Patent # 8,066,967, November 29, 2011.
121. J. Zhang and D. Chen, "Differential mobility particle sizers for nanoparticle characterization," Nanotechnol. Eng. & Med., vol. 5, no. 2, Article ID 020801-1, 9 pp., 2014.
122. H. Moosmuller, R.K. Chakrabarty, and W.P. Arnott, "Particle separation," Reno, NV, US Patent # 7,931,734, April 26, 2011.
123. M.R. Zachariah, M. Li, and G.W. Holland, "Pulsed-field differential mobility analyzer system and method for separating particles and measuring shape parameters for non-spherical particles," Univ. of Maryland, College Park, MD, US Patent # 9,677,984, June 13, 2017.
124. D.P. Brown, A.G. Nasibulin, E.I. Kauppinen, and D. Gonzalez, "Method for separating high aspect ratio molecular structures," Finland, US Patent # 8,871,295, October 28, 2014.
125. T. Butunoi ..... and A. Iuga, "Electric and electronic equipment of a research-oriented electrostatic separator," Proc. 12th Int. Conf. on Optimization of Electrical and Electronic Equipment, IEEE, pp. 639-645, 2010.
126. L. Dascalescu ..... and A. Samuila, "Electrostatic separation processess," IEEE Industry Applications Magazine, November/December, pp. 19-25, 2004.
127. A. Iuga, L. Dascalescu, R. Morar, I. Csorvassy, and V. Neamtu, "Corona-electrostatic separators for recovery of waste non-ferrous metals," Electrostatics, vol.23, pp. 235-243, 1989.
128. A. Yuga, L. Dascalescu, R. Morar, A. Samuila, and I. Cuglesan, "Electrostatic shape separation of flake mica from pegmatite," Magnetic and Electrical Separation, vol. 6, pp. no. 3,135-149, 1995. [Open Access Pub, licensed under https://creativecommons.org/licenses/by/3.0/ ; Images modified].
129. T. Takahashi and K. Tabei, "Electrostatic sorting apparatus," Japan, US Patent # 4,374,727, February 22, 1983.
130. "Laboratory electrostatic separator: Model EHTP (25) 111-15," Sepor, Inc., Wilmington, CA, https://www.sepor.com/ Accessed September 3, 2020.
131. "High tension electrostatic separator: Model 533," Eriez Manufacturing Co., Erie, PA, https://www.eriezlabequipment.com/ Accessed September 3, 2020.

132. “Laboratory mineral separator: OreKinetics Corona Stat; Model 100,” ALS Ltd., QLD, Australia, http://www.alsglobal.com/ Accessed September 3, 2020.
133. P.G. Collins and P. Avouris, “Nanotubes for electronics,” Scientific American, vol. 283, no. 6, pp. 62-69, 2000.
134. S.J. Hales ..... and P.T. Lillehei, “Nanoparticle hybrid composites by RF plasma spray deposition,” NASA Langley Research Center, Hampton, VA, US Patent # 9,963,345, May 8, 2018.

REPORT DOCUMENTATION PAGE

Form Approved
OMB No. 0704-0188

1. REPORT DATE *(DD-MM-YYYY)*	2. REPORT TYPE	3. DATES COVERED *(From - To)*
09/01/2021	TECHNICAL PUBLICATION	

4. TITLE AND SUBTITLE

Radio Frequency Plasma Synthesis of Boron Nitride Nanotubes (BNNTs) for Structural Applications: Part III

5a. CONTRACT NUMBER

5b. GRANT NUMBER

5c. PROGRAM ELEMENT NUMBER

6. AUTHOR(S)

Hales, Stephen J.; Domack, Christopher S.; Jensen, Brian J.; Messick, Peter L.

5d. PROJECT NUMBER

5e. TASK NUMBER

5f. WORK UNIT NUMBER

596118.04.27.23

7. PERFORMING ORGANIZATION NAME(S) AND ADDRESS(ES)

NASA Langley Research Center
Hampton, VA 23681-2199

8. PERFORMING ORGANIZATION REPORT NUMBER

9. SPONSORING/MONITORING AGENCY NAME(S) AND ADDRESS(ES)

National Aeronautics and Space Administration
Washington, DC 20546-001

10. SPONSOR/MONITOR'S ACRONYM(S)

NASA

11. SPONSOR/MONITOR'S REPORT NUMBER(S)

NASA/TP-20210011627

12. DISTRIBUTION/AVAILABILITY STATEMENT

Unclassified - Unlimited
Subject Category
Availability: NASA STI Program (757) 864-9658

13. SUPPLEMENTARY NOTES

This report represents the final installment of a trilogy addressing induction plasma synthesis and post-synthesis processing of mass quantities of BNNTs.

14. ABSTRACT

The emergence of commercial quantities of BNNTs facilitates the exploration of structural material applications. BNNT-reinforced composites must exhibit extraordinary mechanical properties in order to justify the cost premium. Prevailing theory indicates that suitable BNNTs must possess an aspect ratio (AR= length/diameter) approaching 10,000 to provide effective discontinuous reinforcement under tensile loading. A survey of commercial products shows that although the quantities are sufficient, lots of uniform morphology are unavailable. Therefore, the opportunity exists to supplement procedures either during synthesis operations or post-synthesis processing in order to deliver homogeneous batches of hig

15. SUBJECT TERMS

Radio frequency plasma synthesis, Boron nitride nanotubes (BNNTs), Electrostatic separation, Fractionation, Aspect ratio, Metal matrix composites, Structural materials

16. SECURITY CLASSIFICATION OF:			17. LIMITATION OF ABSTRACT	18. NUMBER OF PAGES	19a. NAME OF RESPONSIBLE PERSON
a. REPORT	b. ABSTRACT	c. THIS PAGE			HQ - STI-infodesk@mail.nasa.gov
U	U	U	UU	58	19b. TELEPHONE NUMBER *(Include area code)* 757-864-9658